Available online at www.sciencedirect.com

ScienceDirect

Geochimica et Cosmochimica Acta xxx (2018) xxx–xxx

Geochimica et Cosmochimica Acta

www.elsevier.com/locate/gca

Microbially mediated nitrate-reducing Fe(II) oxidation: Quantification of chemodenitrification and biological reactions

Tongxu Liu [a,1], Dandan Chen [a,b,d,1], Xiaobo Luo [a,b,d], Xiaomin Li [c], Fangbai Li [a,*]

[a] *Guangdong Institute of Eco-environmental Science & Technology, Guangdong Key Laboratory of Integrated Agro-environmental Pollution Control and Management, Guangzhou 510650, PR China*

[b] *Guangzhou Institute of Geochemistry, Chinese Academy of Sciences, Guangzhou 510640, PR China*

[c] *The Environmental Research Institute, MOE Key Laboratory of Theoretical Chemistry of Environment, South China Normal University, Guangzhou 510006, PR China*

[d] *University of Chinese Academy of Sciences, Beijing 100049, PR China*

Received 22 November 2017; accepted in revised form 30 June 2018; available online xxxx

Abstract

Redox reactions between iron and nitrogen drive the global biogeochemical cycles of these two elements and, concomitantly, change the fate of nutrients in and the mineralogy of the cycles. The microbially mediated NO_3^--reducing Fe(II) oxidation process (NRFO) plays a key role in Fe/N interactions under neutral-anoxic conditions. Microbially mediated NRFO was considered a biological process, yet recently it has been documented that chemical mechanisms are also at play. However, the relative contributions of biological processes and chemical processes to Fe(II) oxidation remain largely unquantified owing to the co-occurrence of the reactions. Herein, the kinetics and secondary minerals of microbially mediated NRFO by *Pseudogulbenkiania* sp. strain 2002 and *Acidovorax* sp. strain BoFeN1 were investigated with acetate as electron donor unless otherwise stated. The results of Cells + NO_3^- suggested the two strains could biologically reduce NO_3^- to NO_3^-/NO_x/N_2O/N_2 and concomitantly oxidize acetate and result in cell growth. Fe(II) oxidation and NO_3^- reduction occurred simultaneously in the presence of Fe(II) (Cells + Fe(II) + NO_3^-). For strain BoFeN1, the presence of Fe(II) slightly enhanced the NO_3^- reduction, acetate consumption, and cell growth, all of which were substantially retarded by Fe(II) for strain 2002. When compared with the microbial nitrite reduction, the relatively higher rate of chemical reaction between NO_2^- and dissolved Fe(II) confirmed the occurrence of chemodenitrification in the microbially mediated NRFO processes. After 5 days' incubation, no green rust was observed, and lepidocrocite, goethite, and magnetite were observed with the Cells + Fe(II) + NO_3^- treatment, but only goethite was found with the Fe(II) + NO_2^-. The spectra for the EPSs + Fe(II) treatment suggested that the oxidized *c*-Cyts in the EPSs could oxidize Fe(II), which show the theoretical capability of taking electrons from Fe(II) into the cells via *c*-Cyts. A brief model was established by combining the verified reactions of (1) biological reduction of NO_3^- to NO_2^-/NO_x/N_2O/N_2, (2) Fe(II) oxidation by NO_2^-, and (3) Fe(II) oxidation by *c*-Cyts in EPSs. Based on the model, the rate constant of Fe(II) oxidation by *c*-Cyts in EPSs was derived. For nitrite reduction, the relative contribution of biological processes to the nitrite reduction was higher than that of chemodenitrification. For Fe(II) oxidation, the relative contribution of the chemical process via nitrite to Fe(II) oxidation was higher than that of biological processes. These findings provide a

* Corresponding author.
E-mail address: cefbli@soil.gd.cn (F. Li).

[1] These authors contributed equally to this work.

https://doi.org/10.1016/j.gca.2018.06.040

quantitative interpretation of the chemodenitrification and biological reactions in the microbially mediated NRFO processes, which could assist the mechanistic understanding of the global biogeochemical cycles of iron and nitrogen in subsurface environments.

Keywords: Nitrate reduction; Fe(II) oxidation; Chemodenitrification; Biological process

1. INTRODUCTION

Iron is the fourth most abundant element in the Earth's crust as well as the most prevalent redox-active metal in the biosphere (Croal et al., 2004; Kappler and Straub, 2005). The oxic-anoxic interfaces such as groundwater seeps, freshwater lake sediments and plant rhizosphere are the active areas of iron cycle (Neubauer et al., 2002; Emerson et al., 2010). The iron cycle mediated by biological and chemical processes impacts the fate of pollutants and toxic heavy metals (Weber et al., 2006a, 2006b). Whereas Fe(II) can be oxidized by O_2 via chemical processes under oxic conditions (Emerson et al., 2010), Fe(II) oxidation occurs under anoxic conditions as well in the presence of oxidants (e.g., NO_2^- and MnO_2) via biotic-abiotic coupling processes (Hedrich et al., 2011; Picardal, 2012; Roden, 2012). The biological processes of Fe(II) oxidation at circumneutral pH are mediated by microaerophilic Fe(II)-oxidizing bacteria with low O_2 concentrations, by anaerobic phototrophic Fe(II)-oxidizing bacteria with light, by nitrate-reducing Fe(II) oxidation bacteria under anoxic conditions (Hedrich et al., 2011; Melton et al., 2014). Under anoxic conditions, NRFO bacteria, which are not restricted to environment with light, is supposed to be more abundant than phototrophic bacteria (Kappler and Straub, 2005). It was reported that NRFO bacteria were successfully enriched from marine, spring, groundwater, brackish or freshwaters sediments (Hafenbradl et al., 1996; Emerson et al., 2010; Sorokina et al., 2012). Given the importance of Fe and N cycles in natural subsurface environments, the chemical/biological reactions between Fe and N may be very dominant processes under anoxic conditions (Li et al., 2012; Liu et al., 2014b; Melton et al., 2014), which drive the biogeochemical cycles of iron and nitrogen and, concomitantly, change the fate of nutrients in and the mineralogy of such cycles (Borch et al., 2010; Li et al., 2016a, 2016b; Sun et al., 2016; Xiu et al., 2016). Furthermore, it was reported that nitrate-reducing Fe(II)-oxidizing bacteria can lead to the co-precipitation or adsorption of toxic heavy metals, metalloids and radionuclides in association with the biogenic Fe(III) oxides (Weber et al., 2006a, 2006b; Li et al., 2016a, 2016b; Xiu et al., 2016). Microbially mediated NRFO is considered to play a key role of the Fe/N interactions under neutral-anoxic conditions (Straub et al., 2004; Konhauser et al., 2011; Smith et al., 2017), but the underlying mechanism for this process is largely unknown. Because a direct chemical reaction between nitrate and Fe(II) is unlikely to occur (Ottley et al., 1997), denitrification coupled with Fe(II) oxidation mainly is mediated by nitrate-dependent Fe(II)-oxidizing bacteria, which were discovered more than two decades ago (Straub et al., 1996). It was considered previously that microbially mediated NRFO was only a biological process (Ratering and Schnell, 2001; Kappler et al., 2005; Kumaraswamy et al., 2006). However, almost all the reported bacteria capable of Fe(II) oxidation can directly reduce nitrate via denitrification pathways (Hedrich et al., 2011; Zhang et al., 2012; Etique et al., 2014), and the intermediates of denitrification (i.e., nitrite) can chemically oxidize Fe(II) quickly (Klueglein et al., 2015; Ishii et al., 2016). Therefore, the question was raised whether and to what extent the observed Fe(II) oxidation is enzymatically driven (biological processes) or occurring because of the oxidation via nitrite/NO (chemical processes) (Schaedler et al., 2017; Chen et al., 2018).

Regarding the chemical reactions between Fe(II) and NO_3^-/ NO_2^-/NO/N_2O, although the redox potential of all Fe(III)/Fe(II) pairs, ranging from −314 mV to 14 mV, is more negative than that of all redox pairs in the nitrate reduction pathway (NO_3^-/NO_2^-, +430 mV; NO_2^-/NO, +350 mV; NO/N_2O, +1180 mV; N_2O/N_2, +1350 mV) (Straub et al., 2001; Weber et al., 2006a), it was confirmed that nitrate cannot be directly reduced by Fe(II) without a catalyst (Hansen et al., 1996; Ottley et al., 1997; Hansen et al., 2001). The process of chemical Fe(II) oxidation by nitrate can be accelerated by a number of catalysts, such as Cu^{2+}, iron oxides, and hydroxides, and even microbial surfaces (Coby and Picardal, 2005; Rancourt et al., 2005). The chemical oxidation of Fe(II) by nitrite was discovered several decades ago (Moraghan and Buresh, 1976). Because most bacteria that mediate NRFO can reduce nitrate to nitrite and other intermediates, the reaction between nitrite and Fe(II) may play a more important role in the microbe-Fe(II)-nitrate system, which may have been largely overlooked before (Ratering and Schnell, 2001; Kappler et al., 2005; Weber et al., 2006b). The chemical Fe(II) oxidation by nitrite in the microbe-Fe(II)-nitrate system has attracted great attention very recently (Picardal, 2012; Klueglein and Kappler, 2013). In addition, no matter how Fe(II) oxidation occurs, Fe(II)-Fe(III) intermediate minerals, such as green rust and siderite, may be produced (Schädler et al., 2009; Miot et al., 2009a, 2009b, 2014; Pantke et al., 2012; Etique et al., 2014). It has been proved that the structural Fe(II) in green rust and siderite are more reactive than the dissolved Fe(II) for nitrite reduction (Rakshit et al., 2008, 2016; Grabb et al., 2017). The effects of ligands on the Fe(II) oxidation process also have been explored, which suggested that strong organic ligands, such as citrate, can substantially enhance the chemical oxidation of Fe(II) by nitrite in the microbe-Fe(II)-nitrate system (Pham and Waite, 2008; Kopf et al., 2013). Therefore, the importance of the chemical reaction between Fe(II) and nitrite is

Please cite this article in press as: Liu T., et al. Microbially mediated nitrate-reducing Fe(II) oxidation: Quantification of chemodenitrification and biological reactions. *Geochim. Cosmochim. Acta* (2018), https://doi.org/10.1016/j.gca.2018.06.040

necessarily highlighted in studies of microbially mediated NRFO (Klueglein and Kappler, 2013; Kopf et al., 2013).

Regarding the biological reactions involving Fe(II) and NO_3^-, most bacteria that can mediate NRFO are mixotrophic and require organic co-substrates, such as acetate, to continually oxidize Fe(II) and reduce nitrate (Melton et al., 2014; Laufer et al., 2016). This situation arouses suspicion as to whether Fe(II) oxidation is enzymatically catalyzed or merely a chemical reaction caused by reactive N intermediates of heterotrophic nitrate reduction (Klueglein et al., 2014; Nordhoff et al., 2017). Furthermore, it was observed that 90% of nitrate-reducing bacteria can oxidize Fe(II) with nitrate and organic substrates (Benz et al., 1998; Klueglein et al., 2014; Liu et al., 2014a). A few strains were also found to survive under autotrophic growth conditions without any organic substrate, such as *Paracoccus ferrooxidans* BDN-1, and the chemolithoautotrophic NRFO culture KS (Blöthe and Roden, 2009; He et al., 2016; Laufer et al., 2016). While it was reported that *Pseudogulbenkiania* sp. strain 2002 could continuously grow under autotrophic conditions, it could also grow heterotrophically with several simple organic compounds including acetate, propionate, butyrate and so on (Weber et al., 2006b, 2009; Klueglein et al., 2014; Xiu et al., 2016; Chen et al., 2018). Whereas there is no direct evidence to prove the existence of biological Fe(II)-oxidizing processes (Beller et al., 2013; Schaedler et al., 2017), some indirect observations verifying the biological processes have been made (Rentz et al., 2007). Separating the chemical and biological processes in the microbe-Fe(II)-nitrate system can be very challenging (Schmid et al., 2014), yet Kopf et al. (2013) successfully used a kinetic model approach to quantify the chemical Fe(II)-oxidizing process and prove that *Pseudogulbenkiania* sp. strain MAI-1 could biologically oxidize Fe(II) directly. Another similar study revealed that the rate of chemical oxidation of Fe(II) by nitrite in the clay size fraction was three to six times less than the biological oxidation (Shelobolina et al., 2012). It was also observed that structural Fe(II) in nontronite cannot be chemically oxidized by nitrite, but successfully oxidized by nitrate in the presence of *Pseudogulbenkiania* sp. strain 2002 (Zhao et al., 2013, 2017). Despite the lack of direct enzyme evidence for biological Fe(II) oxidation, the differences between the biological and chemical processes involved in the microbe-Fe(II)-nitrate system have been clearly distinguished (Chen et al., 2018).

During the processes of microbially mediated NRFO, it has been proposed that electrons from Fe(II) go through the electron transfer chain, and finally are accepted by nitrate or its intermediates (Liu et al., 2016; He et al., 2017). It has been proposed that the electrons from Fe(II) are directly transferred to enzymes, such as a dedicated Fe(II) oxidoreductase, nitrate reductase, and cytochrome bc_1 complex (Bird et al., 2011; Carlson et al., 2012; Han et al., 2017; Liu et al., 2017a). The cytochrome *c* of strain 2002 is reduced *in vivo* in the presence of Fe(II) and nitrate, suggesting that at least one type of cytochrome *c* is involved in the electron transfer from Fe(II) to the respiratory chain (Ilbert and Bonnefoy, 2013; Ishii et al., 2016). Although no enzymes involved in microbially mediated NRFO have been identified thus far (Laufer et al., 2016; Schaedler et al., 2017), it was reported that *c*-type cytochromes (*c*-Cyts) of iron-oxidizing bacteria were also involved in the electron transfer between Fe(II) and cell membranes (Weber et al., 2009; Liu et al., 2012; David et al., 2013). Hence, the characterization of *c*-Cyts and their roles in Fe(II) oxidation will be essential for understanding the contributions of biological processes to microbial Fe(II) oxidation (Han et al., 2016; Liu et al., 2017b; Luo et al., 2017). Fortunately, a new spectrophotometer with lower detection limits was recently developed, enabling investigation of the reaction between ferrous ions and *c*-Cyts in intact Fe(II)-oxidizing bacteria (*Leptospirillum ferrooxidans*) under anoxic conditions (Blake and Griff, 2012; Blake et al., 2016). Using this spectrophotometer, the *in situ* spectral kinetics of *c*-Cyts (cytochrome 579) in iron-oxidizing bacteria was successfully examined (Matsuno et al., 2009). Whereas the underlying mechanisms of key proteins mediating electron transfer have not been well characterized, *in situ* spectroscopy is a very promising tool for disclosing the enzymatic mechanisms given the nature of this method for directly observing key proteins (*c*-Cyts) (Nakamura et al., 2009; Luo et al., 2017).

Based on the current understanding of the chemical and biological processes, the kinetics, secondary minerals, and protein reactions of the system of microbially mediated NRFO by two model bacterial strains were comprehensively investigated. The aims of this study were to (1) examine the kinetics of nitrate reduction and Fe(II) oxidation for biological and chemical processes; (2) confirm the occurrence of chemodenitrification and biological reactions; (3) examine the protein reactions using the UV–Vis spectral method; and (4) quantify the relative contributions of chemodenitrification and biological reactions. This study may be helpful for comprehensively interpreting the roles of biological and chemical processes involved in microbially mediated NO_3^--reducing Fe(II) oxidation.

2. MATERIALS AND METHODS

2.1. Bacterial cultivation and chemicals

Acidovorax sp. strain BoFeN1 is a chemoorganotrophic, nitrate-reducing Fe(II)-oxidizing β-proteobacterium that was isolated from Lake Constance littoral sediments (Kappler et al., 2005). *Pseudogulbenkiania* sp. strain 2002 was isolated from a nitrate-dependent Fe(II)-oxidizing most-probable-number enumeration series initiated from sediments collected from a freshwater lake on the Southern Illinois University campus in Carbondale, Illinois (Weber et al., 2006b). Piperazine-N,N′-bis(2-ethanesulfonic acid) (PIPES) (≥99.0%) and $FeCl_2{\cdot}6H_2O$ (≥99.0%) were purchased from Sigma-Aldrich Co. (USA). $Na^{15}NO_3$ (^{15}N at 98+%) was purchased from Cambridge Isotope Laboratories, Inc. (USA). Na_2-EDTA·$2H_2O$ (ethylenediaminetetraacetic acid disodium salt dehydrate, 98%, AR) was purchased from Aladdin (China). Standard horse heart *c*-Cyts (95%, SDS-PAGE and spectral assay), with a molecular mass of 12,384 Da, was obtained from Sigma Chemical Co. (China). Other chemical reagents for cell growth

Please cite this article in press as: Liu T., et al. Microbially mediated nitrate-reducing Fe(II) oxidation: Quantification of chemodenitrification and biological reactions. *Geochim. Cosmochim. Acta* (2018), https://doi.org/10.1016/j.gca.2018.06.040

medium and kinetics experiments were of analytical grade and purchased from Guangzhou Chemical Reagent Factory, China.

An oxygen-free, 30 mM PIPES buffered freshwater mineral medium (pH 7.0) was used in all cultivation studies of the two nitrate-reducing Fe(II)-oxidizing bacteria. For the freshwater mineral medium, the following amounts of salts and other compounds were mixed thoroughly in 1 L of distilled water: 0.3 g of NH_4Cl, 0.3 g of NaCl, 0.42 g of $MgCl_2{\cdot}6H_2O$, 0.14 g KH_2PO_4, 0.1 g $CaCl_2{\cdot}2H_2O$, 10 mL vitamin solution, and 10 mL trace element solution (Pantke et al., 2012). The vitamin and trace mineral solutions were prepared as previously described (Weber et al., 2009). For routine cultivation of the two nitrate-reducing Fe(II)-oxidizing bacteria, according to the literature (Kappler et al., 2005; Miot et al., 2009a), sodium nitrate (10 mM) and sodium acetate (5 mM) were added as the electron acceptor and donor, respectively. The bacteria were anaerobically cultured to the early stationary growth phase, then harvested via centrifugation (6000 $\times g$, 10 min), washed twice with anoxic (100% N_2 atmosphere) PIPES buffer, and resuspended to serve as an inoculum for the following experiments (Zhao et al., 2013). However, the bacteria used for isotopic tracing experiments with ^{15}N-labeled $NaNO_3$ (NO_3^-) were washed twice with anoxic (100% He atmosphere) PIPES buffer (Ding et al., 2014).

2.2. Experimental setup

Serum bottles (58 mL) were washed with 1 M HCl and distilled water prior to sterilization via autoclaving. Into each bottle, 20 mL of sterile anoxic PIPES (30 mM, pH 7.0) was added (sparged with 100% N_2 for at least 30 min). The bottles were sealed with butyl stoppers and crimped, and then transferred into an anaerobic chamber (Plas-Labs, USA, H_2/N_2 (1/99, v/v)). A Fe(II) stock solution (1 M) was prepared by adding $FeCl_2{\cdot}6H_2O$ to anoxic (100% N_2 headspace) distilled deionized water and then filtering (0.22 μm, cellulose nitrate, Millipore) the mixture in an anaerobic chamber. Other stock solutions were prepared in the same way (Kappler et al., 2005). However, 100% N_2 was replaced by 100% He for the isotopic tracing experiment with ^{15}N-labeled $NaNO_3$. Serum bottles with 20 mL PIPES were amended with Fe(II) (5 mM) as the electron donor, nitrate (5 mM) as the electron acceptor, and acetate (2 mM) as an organic co-substrate, and then inoculated with the prepared washed-cell suspensions. Three different biotic treatments were applied: Cells + Fe(II) + NO_3^-, Cells + NO_3^-, and Cells + NO_2^-. All trials were conducted in triplicate and incubated at 30 °C in the dark. For the abiotic treatment (Fe(II) + NO_2^-), bottles containing PIPES were amended with Fe(II) (5 mM), nitrite (3 mM), and acetate (2 mM). For the isotopic tracing experiments with ^{15}N-labeled $NaNO_3$, two treatments (Cells + Fe(II) + NO_3^- and Cells + NO_3^-) were applied.

2.3. Analytical methods

During the incubation period, triplicate bottles were used to quantify the dissolved Fe(II), nitrate, nitrite, N_2O, and NH_4^+. The headspace gas of each serum bottle was sampled using a syringe to determine the total concentration of N_2O (Chen et al., 2018). The N_2O concentration was measured via a Techcomp GC7900 gas chromatograph using ECD detectors. For quantification of total Fe(II), 100 μL of culture suspension was withdrawn and dissolved in 900 μL of 40 mM sulfamic acid (pH approximately 1.8) for 1 h on a rotary shaker at 180 rpm at 26 °C in an anoxic chamber (Klueglein and Kappler, 2013; Li et al., 2009). Total Fe(II) was determined by the 1,10-phenanthroline method. For NO_3^-, NO_2^-, and NH_4^+ measurements, samples were fully exposed to O_2 to rapidly oxidize Fe(II), centrifuged at 8000 $\times g$ for 5 min to remove cells and oxides, and then filtered through a 0.22 μm membrane before analysis (Li et al., 2016a, 2016b). The control experiments with nitrate/nitrite with/without Fe(II) after exposure to O_2 (Fig. S4) suggested no significant effect was found for the measurement of nitrate and nitrite, and the method to treat samples for measuring nitrate/nitrite was reliable under this experimental condition. The concentrations of NO_3^-, NO_2^-, and NH_4^+ were quantified using a Continuous Flow Analyzer (SAN++, Skalar). Samples were buffered at pH 8.2 and passed through a column containing granulated copper-cadmium to reduce nitrate to nitrite. Nitrite was quantified by diazotizing with sulfanilamide and coupling with N-(1-naphthyl)ethylenediamine dihydrochloride to form a highly colored azo dye, which was measured at 540 nm (Chen et al., 2018). The ammonia levels in the samples were determined using the modified Berthelot reaction, which formed a green colored complex that was measured at 660 nm (Li et al., 2015). The concentration of acetate was determined by ion chromatography (DionexICS-90) with an ion column (IonPac AS14A 4 × 250 mm).

Supplementary data associated with this article can be found, in the online version, at https://doi.org/10.1016/j.gca.2018.06.040.

For the isotopic tracing experiments with ^{15}N-labeled $NaNO_3$ (NO_3^-), only initial and final samples were analyzed. Besides NO_3^-, NO_2^-, N_2O, and NH_4^+, ^{15}N-N_2 was also analyzed. Before sampling, each vial was shaken vigorously to equilibrate the gas between the dissolved and gaseous phases. For analysis of ^{15}N-N_2, 12 mL gas samples were immediately collected using gastight syringes and then injected into 12 mL pre-evacuated glass vials (Exetainer, Labco, U.K.). To prevent atmospheric contamination, these sampling processes were conducted in a He-filled anaerobic chamber (Pyramid, Asone, Japan; He 100%). The ^{15}N enrichment in N_2 was determined via isotope ratio mass spectrometry (IRMS, Thermo Finnigan Delta V Advantage, Bremen, Germany) coupled with a GasBench II. Headspace N_2 concentration was measured using an Agilent 7890 gas chromatograph (Santa Clara, CA, USA) (Ding et al., 2014). $^{15}N_2$ concentration was calculated as the product of N_2 concentration and ^{15}N-N_2 atom % excess above its natural abundance (Lewicka-Szczebak et al., 2013; Mulvaney, 1984; Xi et al., 2016).

Biogenic and abiogenic mineral samples were collected from the incubations via filtration inside the anoxic chamber. Samples were filtered onto 0.22 μm filters (VCTP Millipore Isopore), washed twice with deoxygenated DDI

water, and dried in the anoxic chamber. Then, the dry minerals were characterized. The morphology was investigated using scanning electron microscopy (SEM, ProX, Phenom). For structural analysis of minerals, an X-ray diffractometer (XRD, D8 ADVANCE, Bruker) using Cu Kα radiation was utilized with a diffraction angle range of $2\theta = 20$–$80°$. The scan speed was 0.2° per minute, and the step size was 0.01°. MDI Jade 7 software was used for the identification of mineral phases. This software utilizes the International Center for Diffraction Data Powder Diffraction File Database (ICDD PDF-2, Sets 1-46, 1996) as a reference source (Chen et al., 2018).

2.4. Spectral measurement of *c*-Cyts

The diffuse transmittance UV–Vis spectra (DT UV–Vis) of *c*-Cyts in the living cells and in the extracellular polymeric substances (EPSs) of these two strains were measured by an Olis CLARiTY VF spectrophotometer (On-Line Instrument Systems, Inc., Bogart, GA, USA) in an anoxic chamber (Plas-Labs, USA, H_2/N_2 (1/99, v/v)). The *c*-Cyts were extracted from the bacterial cells using an EDTA method, as previously described (Cao et al., 2011). The cells were resuspended in 0.9% NaCl and mixed with 2% Na_2-EDTA in 0.9% NaCl (pH 7.0). The mixture was incubated overnight at 4 °C. After that, cells were pelleted by centrifugation at 5000 ×*g* and 4 °C for 20 min, and the EPSs supernatant was filtered through 0.22 μm membrane filters. The EPSs solution was stored at 4 °C before use. Standard horse heart *c*-Cyts was also measured (Liu et al., 2017a). All spectroscopic and kinetic measurements were conducted in the anoxic chamber. After recording a stable baseline from 300 to 600 nm, identical 5 mL solutions were added to the sample observation cavities of the spectrophotometer. The spectra of the horse heart *c*-Cyts in the living cells and EPSs solutions of these two strains were measured first. To investigate the roles of *c*-Cyts in Fe(II) oxidation, the spectra of *c*-Cyts in EPSs solution with or without Fe(II) (2 μM and 4 μM) and/or nitrate (2 μM) were examined.

2.5. Numerical modeling

The kinetic data of NO_3^-/NO_2^- reduction and Fe(II) oxidation for different treatments were initially fitted with the pseudo-first-order model, and the rate constants were obtained for comparing the different treatments. Based on mechanistic analysis and discussion, the elementary reactions were disclosed and kinetic models based on the verified elementary reactions were established, with the kinetic models fitted to the experimental data over a range of experimental conditions using the program KinTek Explorer (Johnson et al., 2009).

3. RESULTS

3.1. Kinetics of nitrate and nitrite reduction

The kinetics of nitrate reduction by strain BoFeN1 (Fig. 1a) showed that, within 116 h, the initial nitrate

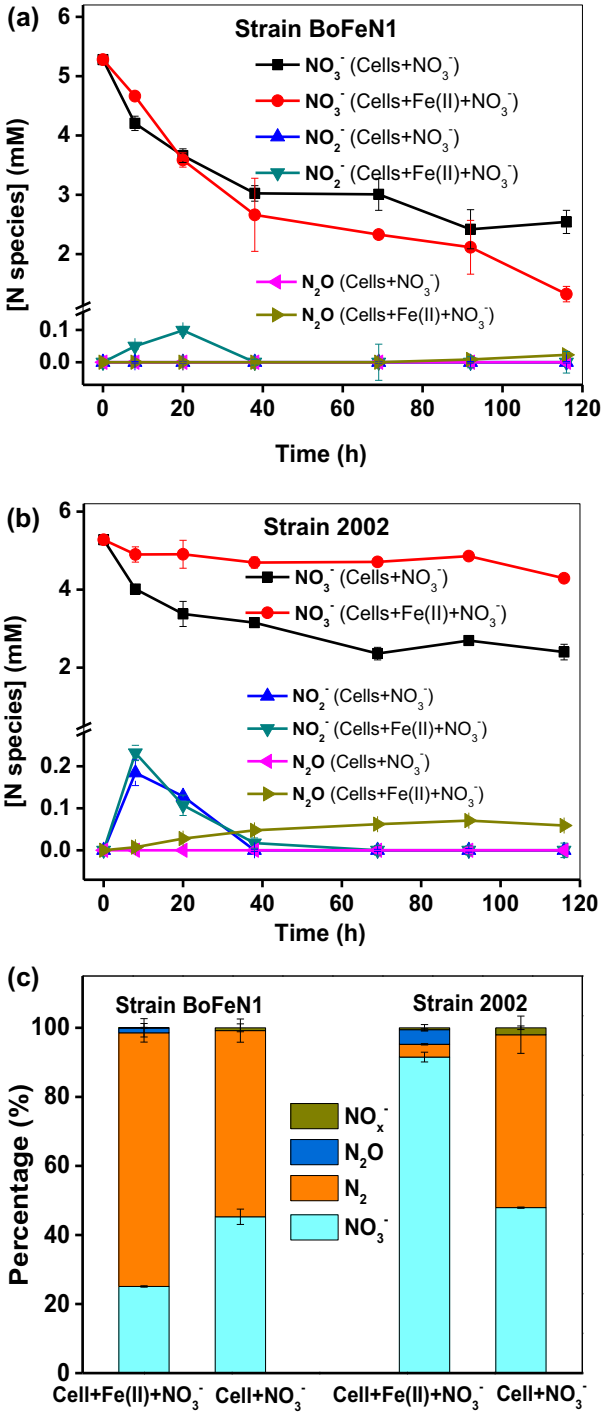

Fig. 1. NO_3^- reduction, NO_2^- formation, and N_2O formation in the treatments with nitrate and ferrous (Cells + NO_3^- and Cells + Fe(II) + NO_3^-). (a) Strain BoFeN1; (b) Strain 2002. (c) Mass balance of nitrogen. The NO_3^-, NO_2^-, and N_2O were observed from the results in Fig. 1a and b, and the N_2 at the end of the incubation was measured based on the ^{15}N of N_2. NO_x represents the nitrogen oxide gases excluding NO_2^-, N_2O and N_2, which was calculated using: NO_3^-–(NO_2^- + N_2O + N_2). Initial concentrations: 4.4 mM Fe(II), 5.3 mM NO_3^-, 4×10^8 strain 2002 cells mL^{-1} or 6×10^8 strain BoFeN1 cells mL^{-1}, and 2 mM acetate in a 30 mM PIPES buffer medium at pH = 7.0. Error bars represent the standard deviation of the mean (n = 3).

(5.3 mM) was reduced to 2.5 mM by cells only (Cells + NO_3^-). The initial nitrate was further reduced to 1.3 mM with the treatment with Fe(II) (Cells + Fe(II) + NO_3^-), suggesting that the presence of Fe(II) slightly enhanced the nitrate reduction, which could be seen from the pseudo-first-order rate constants (k) in Table 1. To further confirm this result, the experiments with a concentration of cells twice as that in Fig. 1 were conducted. The results in Fig. S1 showed an obvious difference of nitrate reduction between Cells + NO_3^- and Cells + Fe(II) + NO_3^-, so it can be confirmed that the presence of Fe(II) enhanced the nitrate reduction by strain BoFeN1. The first-step intermediate of NO_3^- reduction, NO_2^-, was not observed in the Cells + NO_3^- experiment, but a small amount of NO_2^- (~0.1 mM) appeared in the Cells + Fe(II) + NO_3^- experiment within 20 h and then disappeared, suggesting that the presence of Fe(II) may be favorable for NO_2^- accumulation. The gas product (N_2O) was not observed in the Cells + NO_3^- experiment, and only a tiny amount of N_2O (~0.02 mM) was detected at 116 h in the Cells + Fe(II) + NO_3^- treatment.

The kinetics of nitrate reduction by strain 2002 (Fig. 1b) showed a substantial difference in the absence and presence of Fe(II). Within 116 h, whereas the initial nitrate (5.3 mM) was reduced to 2.4 mM by cells only (Cells + NO_3^-), the initial nitrate was only reduced to 4.3 mM in the treatment with Fe(II) (Cells + Fe(II) + NO_3^-). Additionally, the k value of Cells + NO_3^- was more than threefold the k value of Cells + Fe(II) + NO_3^- (Table 1), suggesting that the presence of Fe(II) greatly inhibited the nitrate reduction. The generation of NO_2^-, showing a similar manner in the absence and presence of Fe(II), increased to approximately 0.2 mM at the beginning and then gradually disappeared within 40 h. No N_2O was detected in the Cells + NO_3^- experiment, but the N_2O kept increasing to 0.06 mM during the incubation period in the Cells + Fe(II) + NO_3^- experiment, indicating that the Fe(II) was favorable for N_2O accumulation, which was consistent with the observation for strain BoFeN1.

Because the N_2O and NO_2^- concentrations (Fig. 1a and b, respectively) were very low as compared with the initial NO_3^- concentrations, it was essential to examine the nitrogen mass balance. The NO_3^-, NO_2^-, and N_2O were observed from the results presented in Fig. 1a and b, and the N_2 at the end of the incubation was measured based on the ^{15}N of N_2. The results presented in Fig. 1c show that the total reduced NO_3^- was mainly transformed into N_2, and minute amounts of N_2O and other NO_x compounds were detected. For strain BoFeN1, the presence of Fe(II) enhanced the NO_3^- reduction amount, and the amounts of ^{15}N-N_2 and N_2O increased as well. For strain 2002, whereas the amounts of NO_3^- reduction and ^{15}N-N_2 formation were still relatively high, the presence of Fe(II) greatly inhibited the NO_3^- reduction and N_2 formation. The ^{15}N-N_2 formation amounts for the different treatments were close to the NO_3^- reduction amounts, thus the dominant reactions of NO_3^- reduction in the presence/absence of Fe(II) could be described as $NO_3^- \rightarrow N_2$. Although the reaction of Fe(II) with NO was also an important intermediate product for the entire pathway of nitrate reduction ($NO_3^- \rightarrow NO_2^- \rightarrow NO \rightarrow N_2O \rightarrow N_2$) (Pearsall and Bonner, 1982; Kustin et al., 1966), the NO was not analysed due to the very limited concentration from the mass balance in Fig. 1c.

To clearly illustrate the nitrite reduction by the two strains and Fe(II), the kinetics of nitrite reduction were further examined in the treatments with nitrite and ferrous (Cells + NO_2^- and Fe(II)+ NO_2^-). The kinetics of nitrite reduction by strain BoFeN1, as presented in Fig. 2a, showed that the initial nitrite (4.6 mM) was reduced to 1.94 mM by cells only (Cells + NO_2^-) within 116 h, and 0.16 mM N_2O was formed simultaneously. For strain 2002, the initial nitrite (4.6 mM) was reduced to 1.62 mM by cells only (Cells + NO_2^-), and 0.19 mM N_2O was formed simultaneously. It was noted that the nitrite reduction stopped after 45 h. Based on the results in Fig. S5, the acetate was completely oxidized after 40 h by strain 2002. Hence, the reduction of nitrite by strain 2002 stopped after 45 h due to the complete consumption of acetate. The chemical reduction of nitrite by Fe(II) (Fe(II) + NO_2^-) was conducted as a comparison. The results presented in Fig. 2c show that the initial NO_2^- (2.8 mM) was quickly reduced to 0.8 mM within 110 h, but the N_2O increased slowly to 0.33 mM, suggesting that 1.67 mM nitrogen from NO_2^- was transformed into other nitrogen products. Except N_2O, the other products of nitrite reduction by Fe(II) were NO and N_2 (Kampschreur et al., 2011; Jones et al., 2015). It has been reported that the reaction between Fe(II) and NO was rapid, with N_2O and Fe(II) as products (Kustin et al., 1966; Pearsall and Bonner, 1982). Regarding the pseudo-first-order rate constants (k) listed in Table 1, whereas the k values for strains BoFeN1 and 2002 were very similar, the k value of the chemical treatment (Fe(II) + NO_2^-) was

Table 1
Pseudo-first-order rate constants (k, h^{-1}) of NO_3^-, NO_2^-, Fe(II), acetate degradation, and total proteins during the incubation period.

Strain	Treatment	Pseudo-first-order rate constant (k, h^{-1})				
		NO_3^-	NO_2^-	Fe(II)	Acetate	Protein
BoFeN1	Cells + NO_3^-	0.007 ± 0.001	/	/	0.022 ± 0.005	0.038 ± 0.012
	Cells + NO_2^-	/	0.010 ± 0.001	/	0.002 ± 0.001	~0
	Cells + NO_3^-+Fe(II)	0.011 ± 0.001	/	0.012 ± 0.001	0.026 ± 0.006	0.030 ± 0.008
2002	Cells + NO_3^-	0.010 ± 0.002	/	/	0.083 ± 0.018	0.033 ± 0.011
	Cells + NO_2^-	/	0.011 ± 0.002	/	0.006 ± 0.001	~0
	Cells + NO_3^-+Fe(II)	0.003 ± 0.001	/	0.003 ± 0.000	0.005 ± 0.000	0.008 ± 0.007
None	NO_2^-+Fe(II)	/	0.019 ± 0.002	0.033 ± 0.003	/	/

Please cite this article in press as: Liu T., et al. Microbially mediated nitrate-reducing Fe(II) oxidation: Quantification of chemodenitrification and biological reactions. *Geochim. Cosmochim. Acta* (2018), https://doi.org/10.1016/j.gca.2018.06.040

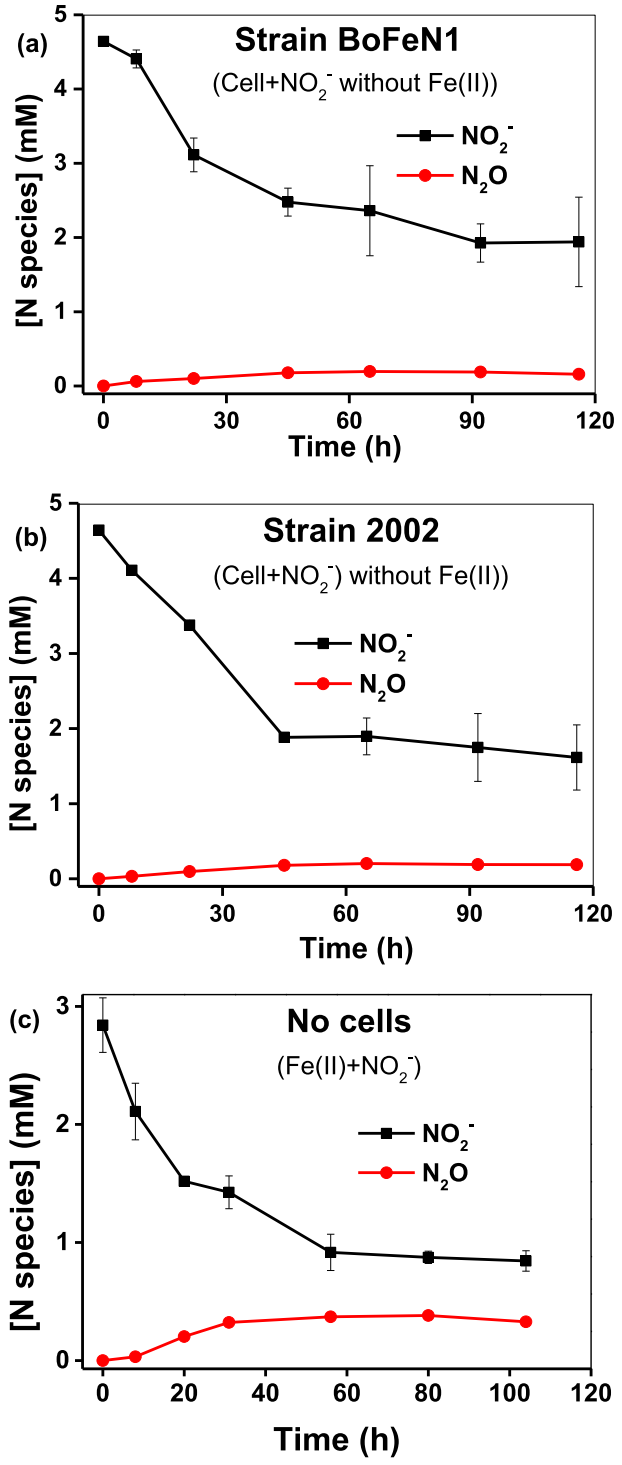

Fig. 2. NO_2^- reduction and N_2O formation in the treatments Cells + NO_2^- and Fe(II) + NO_2^- (a) Strain BoFeN1; (b) Strain 2002; (c) No cells (Fe(II) + NO_2^-). Initial concentrations: 4.4 mM Fe(II), 4.6 mM NO_2^- for Cell + NO_2^- treatment and 2.8 mM NO_2^- for Fe(II) + NO_2^- treatment, 4×10^8 strain 2002 cells mL^{-1} or 6×10^8 strain BoFeN1 cells mL^{-1}, and 2 mM acetate in a 30 mM PIPES buffer medium at pH = 7.0. Error bars represent the standard deviation of the mean (n = 3).

nearly twofold that of the biological treatment (Cells + NO_3^-).

3.2. Kinetics of Fe(II) oxidation and formation of iron minerals

In the presence of strain BoFeN1 and nitrate, the initial Fe(II) concentration (4.4 mM) decreased to 1.3 mM (oxidized 3.1 mM) within 116 h (Fig. 3). Differently, in the presence of strain 2002 and nitrate, just 1.4 mM of the initial Fe (II) was oxidized, suggesting that the Fe(II) oxidation with strain BoFeN1 and NO_3^- is much higher than that with strain 2002 and NO_3^-. Whereas no chemical Fe(II) oxidation was observed in the reaction between nitrate and Fe (II) (data not shown), the initial Fe(II) (4.4 mM) was chemically oxidized by NO_2^- to 0.1 mM within 104 h in the Fe (II) + NO_2^- experiment, indicating that the abiotic Fe(II) oxidation by nitrite was much faster than Fe(II) oxidation in microbially mediated nitrate-reduction Fe(II) oxidation process with strain BoFeN1 or strain 2002. The above kinetics (Figs. 1–3) suggested that Fe(II) oxidation and nitrate reduction in the presence of strain BoFeN1 or strain 2002 occur simultaneously.

Fe(II) oxidation to Fe(III) can result in the formation of iron minerals. The morphology of the solid samples after incubation for 116 h was examined via SEM (Fig. 4). The image in Fig. 4a shows that the minerals via strain BoFeN1 (Cells + Fe(II) + NO_3^-) had very complex shapes, mainly needle-like and rod-like shapes, and some scale-like solids were also observed covering the cells, which might be cell encrustation. The shapes of the minerals via strain 2002 (Cells + Fe(II) + NO_3^-), shown in Fig. 4b, were also very complex but differed from those of strain BoFeN1. More rod-like shapes but less needle-like shapes were observed

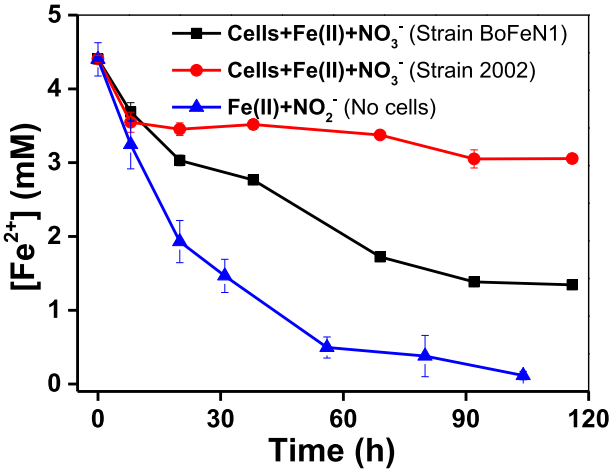

Fig. 3. Fe(II) oxidation in the treatments Cells + Fe(II) + NO_3^- and Fe(II) + NO_2^-. Initial concentrations: 4.4 mM Fe(II), 5.3 mM NO_3^-, 2.8 mM NO_2^- for Fe(II) + NO_2^- treatment, 4×10^8 strain 2002 cells mL^{-1} or 6×10^8 strain BoFeN1 cells mL^{-1}, and 2 mM acetate in a 30 mM PIPES buffer medium at pH = 7.0. Error bars represent the standard deviation of the mean (n = 3).

Please cite this article in press as: Liu T., et al. Microbially mediated nitrate-reducing Fe(II) oxidation: Quantification of chemodenitrification and biological reactions. *Geochim. Cosmochim. Acta* (2018), https://doi.org/10.1016/j.gca.2018.06.040

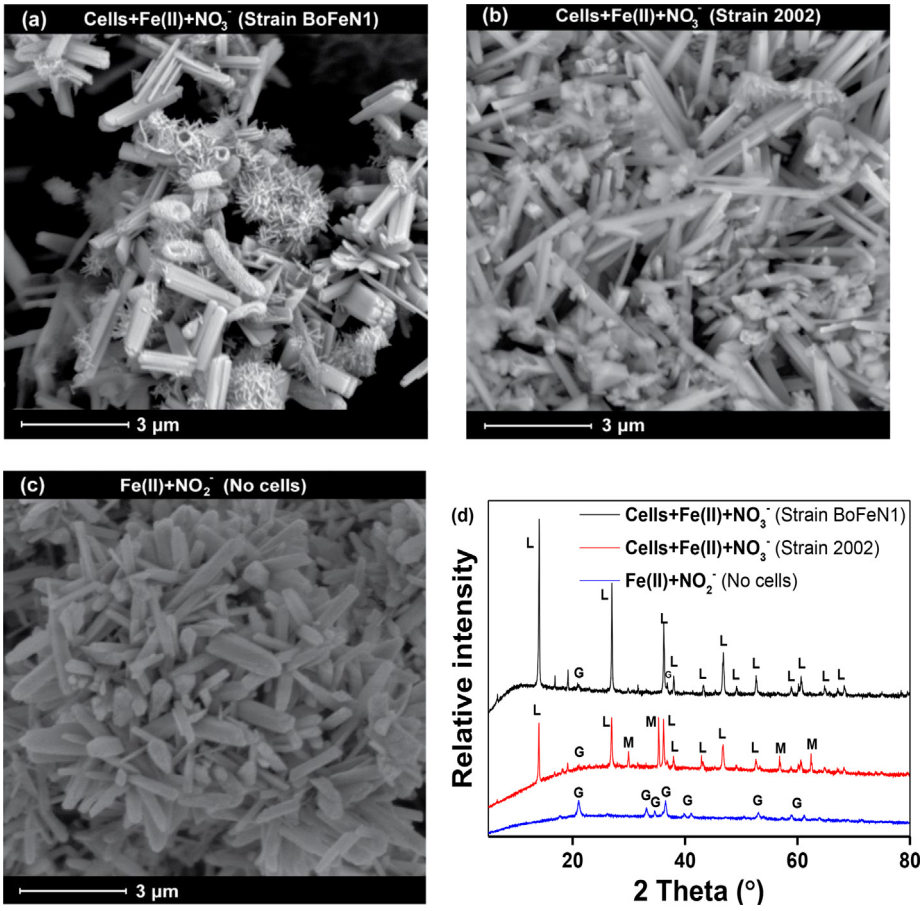

Fig. 4. SEM images of the minerals produced after incubation with the three treatments. (a) Cells + Fe(II) + NO_3^- (strain BoFeN1); (b) Cells + Fe(II) + NO_3^- (strain 2002); (c) Fe(II) + NO_2^- (no cells). (d) XRD patterns of the minerals obtained from these three treatments. "G" strands for goethite, "L" stands for lepidocrocite, "M" stands for magnetite.

compared to those seen in Fig. 4a. Besides, some diamond-shape minerals were also observed in Fig. 4b. The shape of the minerals for the no cell treatment (Fe(II) + NO_2^-) (Fig. 4c) was very uniformly rod-like. The crystal structures of the iron minerals were further characterized by XRD. The results presented in Fig. 4d show that the main Fe (III) minerals via strain BoFeN1 (Cells + Fe(II) + NO_3^-) were lepidocrocite and goethite, and those via strain 2002 were lepidocrocite, goethite, and magnetite. Moreover, the only form of the Fe(III) mineral for the no cell treatment (Fe(II) + NO_2^-) was goethite.

3.3. Kinetics of acetate oxidation and cell growth

Acetate (2 mM) was used as an electron donor for supporting cell growth of the two strains. The time-course changes of acetate accompanying the Fe(II) oxidation and nitrate reduction were examined. The results presented in Fig. 5a show that acetate decreased mostly within 92 h for both treatments with strain BoFeN1 (Cells + Fe(II) + NO_3^- and Cells + NO_3^-), and the degradation curves for both treatments were very similar, suggesting that the influence of Fe(II) on the utilization rate of acetate by strain BoFeN1 could be neglected. Furthermore, cell growth, as indicated by protein concentrations, during the incubations was examined as well. Because it is difficult to enumerate cells in the presence of iron minerals, cell protein concentrations of the Cells + Fe(II) + NO_3^- and Cells + NO_3^- treatments were measured to evaluate the relative changes (Zhao et al., 2013). The results presented in Fig. 5a show that the cell protein concentrations in the two treatments increased gradually until 40 h. The results showed the protein concentration for Cells + Fe(II) + NO_3^- increased slightly as compared to that for Cells + NO_3^- (Fig. 5(a)), indicating that the presence of Fe(II) enhanced the protein production. Furthermore, the enhancement of nitrate reduction by Fe(II) also indicated that nitrate reduction was potentially coupled to the Fe(II) oxidation and cell growth (Figs. 1 and S1). Therefore, the above results suggested that the Fe(II) was very likely to be involved in the enzymatic process.

In Fig. 5b, the residual acetate decreased from 2 mM to 0 mM within 38 h in the treatments with strain 2002 (Cells + NO_3^-), but the presence of Fe(II) (Cells + Fe(II) + NO_3^-) dramatically retarded the acetate degradation, suggesting that Fe(II) had great inhibitory effects on the utilization rate of acetate by strain 2002 and Fe(II) oxidation was not beneficial to the cells of strain 2002. The results of the

Please cite this article in press as: Liu T., et al. Microbially mediated nitrate-reducing Fe(II) oxidation: Quantification of chemodenitrification and biological reactions. *Geochim. Cosmochim. Acta* (2018), https://doi.org/10.1016/j.gca.2018.06.040

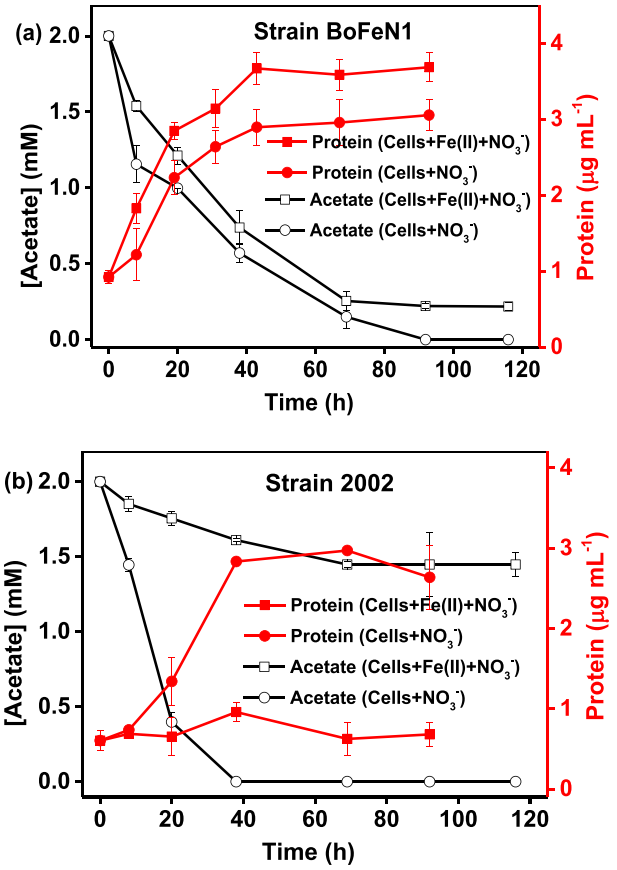

Fig. 5. Time-course changes of the residual acetate concentrations and the cell protein concentrations in the nitrate-reducing Fe(II) oxidation using strains (a) BoFeN1 and (b) 2002. The black open symbols represent the residual acetate concentrations, and the red solid symbols represent the cell protein concentrations. Initial concentrations: 4.4 mM Fe(II), 5.3 mM NO_3^-, 4×10^8 strain 2002 cells mL^{-1} or 6×10^8 strain BoFeN1 cells mL^{-1}, and 2 mM acetate in a 30 mM PIPES buffer medium at pH = 7.0. Error bars represent the standard deviation of the mean (n = 3). (For interpretation of the references to colour in this figure legend, the reader is referred to the web version of this article.)

cell protein concentrations presented in Fig. 5b show that, whereas the cell protein concentrations in Cells + NO_3^- increased quickly from 0.6 μg mL^{-1} to a stable value of ~2.9 μg mL^{-1} within 40 h, the cell protein concentration in Cells + Fe(II) + NO_3^- remained in a narrow range, between 0.60 and 0.95 μg mL^{-1}. These results indicated no significant cell growth of strain 2002 was observed in the presence of Fe(II) and nitrate (Cells + Fe(II) + NO_3^-), which was a different behaviour compared to that of strain BoFeN1.

To compare the electrons from acetate and Fe(II) to those for nitrate reduction, the full electron balance of all the redox species at the end of the reactions was made (Table 2). The results showed that the electrons from electron donors (acetate) were very close to those from electron acceptors (nitrate) for two strains in Cells + NO_3^-, suggesting that most of the electrons from acetate went to the nitrate. In the presence of Fe(II) with strain BoFeN1, the electrons from electron donors (acetate) were obviously less than those from electron acceptors (nitrate), and the total electrons from acetate and Fe(II) were close to the number of electrons that can be accepted by the nitrate present, suggesting that the cells of strain BoFeN1 had the capacity of taking electrons from Fe(II). For strain 2002, the electrons from electron donors (acetate) were almost the same as those from electron acceptors (nitrate), so it remained unclear whether the cells of strain 2002 could take electrons from Fe(II).

3.4. Spectral evidence of *c*-Cyts for Fe(II) oxidation

Because it has been reported that outer membrane *c*-Cyts of iron-oxidizing bacteria were also involved in the extracellular electron transfer between Fe(II) and cell membranes (Weber et al., 2009; Liu et al., 2012; David et al., 2013), the spectra of *c*-Cyts in the living cells and in the EPSs of these two strains were examined. The results presented in Fig. 6a show that a distinct peak appeared at 410 nm in both the EPSs and living cells of strain BoFeN1. As compared with the spectrum of horse heart *c*-Cyts in oxidized form (Liu et al., 2017a), the spectra of the EPSs and living cells were well matched with the oxidized *c*-Cyts, indicating that *c*-Cyts existed in strain BoFeN1, especially in the EPSs or outer membrane of cells. Similarly, the results presented in Fig. 6b show that a distinct peak appeared at 410 nm in both the EPSs and living cells of strain 2002, which indicated that *c*-Cyts existed in strain 2002 as well. The peak intensity of *c*-Cyts in the EPSs was close to that in living cells, suggesting that the *c*-Cyts in the EPSs might be the dominant forms of *c*-Cyts in the living cells.

To investigate the roles of *c*-Cyts in Fe(II) oxidation, the spectra of *c*-Cyts in the presence/absence of Fe(II) and/or nitrate were examined. The results presented in Fig. 7a show that the *c*-Cyts in the EPSs of strain BoFeN1 were in fully oxidized form, but were transformed into fully reduced form, indicated by the peak at 550 nm, after addition of Fe(II) (2 μM and 4 μM). At the same time, the peak

Table 2
The number of electron donors and acceptors for the treatments Cells + NO_3^- and Cells + Fe(II) + NO_3^- at the last time (116 h).

Strain	Treatment	Electron donors (mM e^-)		Electron acceptors (mM e^-)
		Acetate	Fe(II)	NO_3^-
BoFeN1	Cells + Fe(II) + NO_3^-	14.3 ± 0.2	3.1 ± 0.2	19.5 ± 0.6
	Cells + NO_3^-	15.9 ± 0.1	/	14.3 ± 0.9
2002	Cells + Fe(II) + NO_3^-	4.4 ± 0.6	1.34 ± 0.1	4.4 ± 0.3
	Cells + NO_3^-	15.9 ± 0.1	/	14.40 ± 1.0

Please cite this article in press as: Liu T., et al. Microbially mediated nitrate-reducing Fe(II) oxidation: Quantification of chemodenitrification and biological reactions. *Geochim. Cosmochim. Acta* (2018), https://doi.org/10.1016/j.gca.2018.06.040

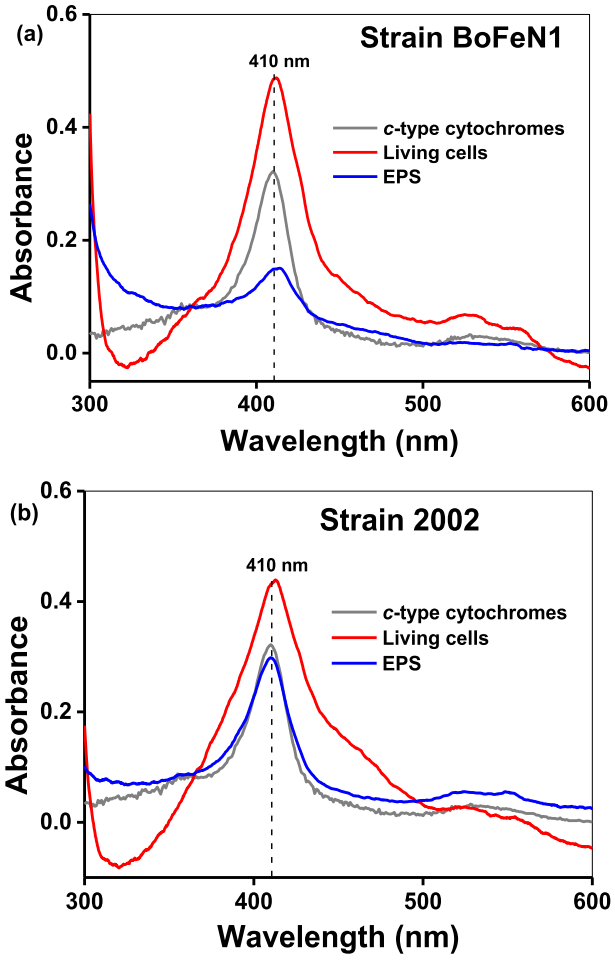

Fig. 6. DT-UV/Vis spectra of the cell suspension and EPSs solution of the two strains. (a) Strain BoFeN1; (b) Strain 2002. The inserts represented the specific absorbance peaks at the wavelength 470–600 nm of *c*-Cyts in the EPSs solution.

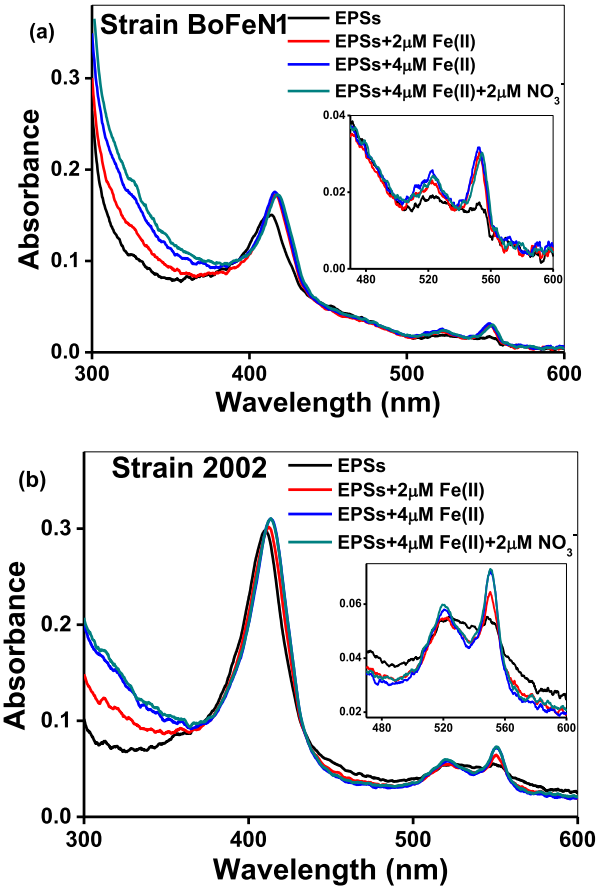

Fig. 7. DT-UV/Vis spectra of *c*-Cyts in the EPSs solution of the two strains after adding Fe(II) (2 μM and 4 μM) and/or 2 μM NO_3^-. (a) Strain BoFeN1; (b) Strain 2002.

at 410 nm shifted to 415 nm. The peaks at 550 nm with Fe(II) (2 μM and 4 μM) were very close, suggesting that 2 μM Fe(II) was sufficient to reduce most of the *c*-Cyts in the EPSs of strain BoFeN1. After further addition of 2 μM NO_3^- to the treatment (EPSs + 4 μM Fe(II)), no clear change was observed in the spectrum of the fully reduced *c*-Cyts, suggesting that the reduced *c*-Cyts was unable to reduce nitrate directly. The results presented in Fig. 7b show that the *c*-Cyts in the EPSs of strain 2002 were in fully oxidized form, but were transformed into reduced form, as indicated by the peak at 550 nm, after addition of Fe(II) (2 μM and 4 μM). The peak at 550 nm with 4 μM Fe(II) was obviously higher than that with 2 μM Fe(II), suggesting that 2 μM Fe(II) was not sufficient to reduce all the *c*-Cyts in the EPSs of strain 2002. Hence, the content of *c*-Cyts in the EPSs of strain 2002 should be higher than that of strain BoFeN1. After further addition of 2 μM NO_3^- to the treatment (EPSs + 4 μM Fe(II)), no clear change was observed in the spectrum of the fully reduced *c*-Cyts, suggesting that the reduced *c*-Cyts of strain 2002 was unable to reduce nitrate directly.

4. DISCUSSION

For microbially mediated nitrate-reducing Fe(II) oxidation, owing to the involvement of very fast abiotic Fe(II) oxidation by an intermediate of nitrate bioreduction (nitrite and NO), some studies tend to recognize Fe(II) oxidation as an innate capability of nitrate-reducing bacteria that involves abiotic and biotic reactions (Carlson et al., 2013), and it was suggested that the induction of specific Fe(II) oxidoreductase proteins was not required. However, very recently, He et al. (2017) suggested that the oxidation of dissolved Fe(II) in the periplasm is coupled to the reduction of nitrate or its reduction intermediates by directly donating electrons to the nitrate/nitrite/nitric oxide reductases and other periplasmic redox-active components, or the oxidation is abiotic, using nitrite and nitric oxide as oxidants. It was also suggested that the electron transferring pathways may be diverse and one genetic system is not universally present in every iron-oxidizing bacteria. Therefore, the distinction and quantification of the biological and chemical processes remains unclear. In this study, the abiotic Fe(II) oxidation by nitrite produced from nitrate reduction was verified from the kinetic studies and identification of minerals, and the theoretical capability of taking

Please cite this article in press as: Liu T., et al. Microbially mediated nitrate-reducing Fe(II) oxidation: Quantification of chemodenitrification and biological reactions. *Geochim. Cosmochim. Acta* (2018), https://doi.org/10.1016/j.gca.2018.06.040

electrons from Fe(II) by the proteins on the cells was suggested from the electron balance calculation, the enhancement of nitrate reduction and proteins by Fe(II), and the spectral evidence of iron-oxidizing proteins. Two possible pathways of nitrate reduction coupled with Fe(II) oxidation are proposed: (i) biological metabolism of Fe(II) and nitrate in which Fe(II) is enzymatically oxidized by *c*-Cyts in the EPSs or outer membrane (enzymatic reactions) and (ii) Fe(II) oxidation by biogenic nitrite in which nitrate is first reduced to nitrite by strain BoFeN1 or strain 2002, followed by Fe(II) oxidation by nitrite (chemodenitrification).

4.1. Biological reactions of Fe(II) and nitrate

The kinetic results showed that, whereas an abiotic reaction between nitrate and Fe(II) did not occur, the presence of strain BoFeN1 or strain 2002 could induce substantial nitrate reduction and Fe(II) oxidation. NO_2^-, N_2O, and N_2 were identified as products of chemical nitrate reduction, no obvious NH_4^+ was observed, and Fe(III) minerals (lepidocrocite and goethite) or Fe(II)/Fe(III) minerals (magnetite) were produced. Gibbs free energies of the chemical reactions between nitrate and Fe(II) were calculated (Chen et al., 2018), which showed that the ΔG_r^o of all the reactions were negative, indicating that the chemical reactions might be thermodynamically feasible. However, nitrate cannot be directly reduced by Fe(II) without a catalyst (Picardal, 2012).

Despite the low feasibility of direct Fe(II) oxidation by nitrate, strains BoFeN1 and 2002 may play the role of a catalyst that can obviously facilitate the reaction between Fe(II) and nitrate. Given the negative Gibbs free energies for the reactions between Fe(II) and nitrate, strains BoFeN1 and 2002 might gain energy from the redox reactions between Fe(II) and nitrate. Whereas the enzymes are required to oxidize Fe(II) during biological Fe(II) oxidation, no enzymes involved in Fe(II) oxidation by NO_3^--reducing Fe(II) oxidation bacteria have been identified to date (Laufer et al., 2016). Nevertheless, some Fe (II) oxidation genes (i.e., those for cytochrome *c* and multicopper oxidase) potentially involved in Fe(II) oxidation were also identified (He et al., 2017), and cytochrome *c* of strain 2002 was also confirmed as related to Fe(II) oxidation (Ilbert and Bonnefoy, 2013). Moreover, the reduction potentials of the possible Fe(III)/Fe(II) redox pairs range from −0.314 V to +0.014 V, indicating that electrons can be donated readily to the more electron-positive cytochrome *c* components of the electron transport chain to reduce nitrate (Weber et al., 2006a). Thus, it would be ideal to directly monitor the redox reactions between Fe(II) and *c*-Cyts in the living bacteria cells; however, because of a lack of appropriate techniques, it remained difficult to gain the redox dynamics of *in vivo* *c*-Cyts of Fe(II)-oxidizing bacteria. Some progress has been achieved in very recent studies about the *c*-Cyts in living iron-reducing bacteria by employing diffuse-transmittance UV/Vis spectroscopy (Liu et al., 2016, 2017a, 2017b). Hence, it would be promising to examine the *in situ* redox spectra of *c*-Cyts in living Fe(II)-oxidizing bacteria under anoxic conditions with similar spectral methods. In the current study, the living cells of strains BoFeN1 and 2002 were directly analyzed by employing DT-UV/Vis spectroscopy, and the specific peaks of *c*-Cyts were observed for both strains, confirming that *c*-Cyts were definitely present in the cells of strains BoFeN1 and 2002. To further disclose the roles of *c*-Cyts in biological reactions between Fe(II) and nitrate, the EPSs containing *c*-Cyts were extracted and the reactions between EPSs and Fe(II) were verified in the presence and absence of nitrate. The changes in the redox status of *c*-Cyts in the presence and absence of Fe(II) confirmed that the *c*-Cyts could be abiotically reduced by Fe(II). This provided a phenomenal evidence for the potential capability of taking electrons from Fe(II) by this cytochrome on the cell surface. According to the electron balance results of strain BoFeN1, the enzymatic Fe(II) oxidation could theoretically occur in strain BoFeN1 with nitrate. From the literature (He et al., 2017), many neutrophilic Fe(II)-oxidizing bacteria have extracellular electron transfer (EET) system, which can mediate electron transfer reactions from the cell surface to the inner membrane. For example, *Sideroxydans lithotrophicus* ES-1 contains MtoA, an outer-membrane cytochrome, which works in concert with MtoB and $CymA_{ES\text{-}1}$ to mediate electron transfer from Fe(II) to the inner membrane (Liu et al., 2012). In this study, the extracted EPS contained outer-membrane cytochromes (Cao et al., 2011), which can act as Fe oxidase to directly accept electron from Fe(II).

In addition, the nitrate was not reduced by reduced *c*-Cyts, suggesting that the nitrate reduction via the two strains was not attributed to the *c*-Cyts but to some other functional genes and proteins. From the kinetics of acetate and proteins shown in Fig. 5, cell growth as indicated by the total proteins was dependent on the consumption of the electron donor (acetate). Nitrate as an electron acceptor is essential for cell growth and acetate metabolism for both strains BoFeN1 and strain 2002. While the current data presented did not provide direct evidence that Fe(II) oxidation was coupled to cell growth, the presence of Fe(II) did influence the cell growth and acetate consumption. For strain BoFeN1, the slight enhancement in acetate and proteins were observed in the presence of Fe(II), implying that cell metabolic function was not inhibited by the secondary minerals on the cell surface (Kappler et al., 2005). However, for strain 2002, the presence of Fe(II) remarkably retarded the nitrate reduction, cell growth, and acetate consumption, indicating that Fe(II) or the secondary minerals may have had very negative impacts on the cell metabolic processes (Klueglein et al., 2014).

4.2. Chemodenitrification of Fe(II) and nitrite

The kinetic results showed that the nitrite could chemically oxidize Fe(II) based on the kinetics of the treatment (Fe(II) + NO_2^-). As a result of chemical Fe(II) oxidation, a Fe(III) mineral (goethite) was produced at pH 7. N_2O and N_2 were identified as products of chemical nitrite reduction by Fe(II). The Gibbs free energies (ΔG_r^o) of chemical reactions between Fe(II) and nitrite were very negative (Picardal, 2012), indicating that the chemical reactions between Fe(II) and nitrite were thermodynamically feasible.

Please cite this article in press as: Liu T., et al. Microbially mediated nitrate-reducing Fe(II) oxidation: Quantification of chemodenitrification and biological reactions. *Geochim. Cosmochim. Acta* (2018), https://doi.org/10.1016/j.gca.2018.06.040

Chemical oxidation of Fe(II) by nitrite was discovered several decades ago (Moraghan and Buresh, 1976). Many bacteria can reduce nitrate to nitrite (Emerson et al., 2010; Carlson et al., 2013), therefore reactions between Fe(II) and nitrite may play important roles in the microbially mediated nitrate-reducing Fe(II) oxidation system, which was largely overlooked until recently studied by Klueglein and Kappler (2013). In addition, no N_2O had accumulated in the nitrate reduction by cells only (Cells + NO_3^-), but N_2O had accumulated with the Fe(II) (Cells + Fe(II) + NO_3^-) and abiotic (Fe(II) + NO_2^-) treatments, implying that in addition to biological nitrite reduction, abiotic nitrite reduction by Fe(II) may be involved in the nitrate reduction process. Hence, competition between chemical nitrite reduction and biological nitrite reduction occurred simultaneously in the Cells + Fe(II) + NO_3^- system. The measured nitrite did not reflect the total amount of nitrite formed and reacted but rather the remaining nitrite after some of the nitrite had reacted with Fe(II) or been biologically reduced. Thus, although the amount of nitrite generated by Cells + Fe(II) + NO_3^- was much lower than the total nitrate amount, chemical Fe(II) oxidation by biogenic nitrite may have relatively high contribution to the overall Fe(II) oxidation. Therefore, the importance of the well-confirmed chemical reaction between Fe(II) and nitrite should be highlighted in all the processes involved in microbially mediated NRFO.

4.3. Kinetic model of chemodenitrification and biological reactions

Based on the aforementioned discussion, the chemodenitrification involved in the microbially mediated nitrate-reducing Fe(II) oxidation processes were confirmed, and the two strains also have the theoretical capability of taking electrons from Fe(II) into the cells, though it remained to be shown whether these electrons can be coupled to nitrate reduction. Because the Fe(II) oxidation and nitrate/nitrite reduction occurred via the above consecutive and parallel reactions, it was not possible to describe the elementary reactions by simply fitting the experimental data in Fig. 1 using the typical model (e.g., pseudo-first-order), owing to the complexity of multi-reactants and multi-mechanisms. Because it is very difficult to monitor all the elementary reactions involved in the Fe-N coupling processes, simplified reactions that contained only the dominant reactants were used for the kinetic modeling studies. For nitrate reduction, first nitrate is biologically reduced by cells to nitrite (Rxn. 1), and then nitrite is further reduced to the products (i.e., N_2O, N_2) (Rxn. 2). In the presence of Fe(II), the nitrite also can be chemically reduced by Fe(II) (Rxn. 3); at the same time, Fe(II) is oxidized to Fe(III). It was reasonable to assume that the Fe(II) oxidation by this cytochrome was coupled to nitrate reduction (Rxn. 4), based on the facts that (i) the enhancement of nitrate reduction and cell growth were observed in the presence of Fe(II); (ii) the electron balance showed the electrons from Fe(II) might go to cells; and (iii) the cytochromes in EPS were also able to oxidize the Fe(II).

$$NO_3^- \xrightarrow{k_{bio,1}} NO_2^- \quad k_{bio,1}\left(s^{-1}\right) \qquad \text{(Rxn. 1)}$$

$$NO_2^- \xrightarrow{k_{bio,2}} N_2O \rightarrow N_2 \quad k_{bio,2}\left(s^{-1}\right) \qquad \text{(Rxn. 2)}$$

$$NO_2^- + Fe(II) \xrightarrow{k_{chem}} N_2O \rightarrow N_2 \quad k_{chem}\left(M^{-1}s^{-1}\right) \qquad \text{(Rxn. 3)}$$

$$Fe(II) \xrightarrow{k_{bio,3}} Fe(III) \quad k_{bio,3}\left(s^{-1}\right) \qquad \text{(Rxn. 4)}$$

Based on the calculation from Visual Minteq at pH 7.0, assuming Fe(II) was oxidized to ferrihydrite ($Fe_5HO_8{\cdot}4H_2O$) with the specific surface area (600 $m^2\,g^{-1}$), the adsorbed Fe(II) could only occupy 43.4% of total surface sites (0.35 mM). However, during the whole reaction process, the formation of ferrihydrite started from 0 mM, so the adsorption capacity of Fe(II) should be far less than the initial dissolved Fe(II) (4.4 mM). It is well known that the sorbed Fe(II) reacts faster than free dissolved Fe(II), so the reaction between sorbed Fe(II) and nitrite should also be considered. However, to simplify the model calculation, to simplify the model calculation, the oxidations of sorbed Fe(II) and dissolved Fe(II) was considered together as the oxidation of Fe(II) in the brief model. Since the heterogeneous Fe(II) oxidation might be important in some other cases with high concentrations of sorbed Fe(II), it should be necessary to include the oxidation of sorbed Fe(II) to obtain a more comprehensive model in the future. The reactions (Rxns. 1, 2, and 4) are the first-order kinetic reactions, and the reaction (Rxn. 3) is the second-order kinetic reaction. Hence, the rate expressions for the above four reactions (Rxns. 1–4) can be written as the following four equations (Eqs. 1–4).

$$\frac{d[NO_2^-]}{dt} = k_{bio,2}[NO_2^-] \qquad \text{(Eq. 1)}$$

$$\frac{d[NO_2^-]}{dt} = k_{chem}[Fe(II)][NO_2^-] \qquad \text{(Eq. 2)}$$

$$\frac{d[Fe(II)]}{dt} = k_{bio,3}[Fe(II)] \qquad \text{(Eq. 3)}$$

$$\frac{d[Fe(II)]}{dt} = k_{chem}[Fe(II)][NO_2^-] \qquad \text{(Eq. 4)}$$

The $k_{bio,1}$ and $k_{bio,2}$ represent the first-order rate constants of the biological reductions of nitrate and nitrite, respectively. The k_{chem} represents the second-order rate constant of the chemical reaction between Fe(II) and nitrite. The $k_{bio,3}$ represents the first-order rate constant of the direct enzymatic Fe(II) oxidation by the functional proteins.

Based on Rxns. 1–4 and Eqs. 1–4, the kinetic models for the chemical treatment (Fe(II) + NO_2^-) and biological treatments (Cells + Fe(II) + NO_3^- and Cells + NO– 3) were established. At the fixed pH 7, the chemical reaction between Fe(II) and NO_2^- should be the same as that in biotic treatments, so the rate constant of chemodenitrification could be fixed in the abiotic or biotic-abiotic coupling processes (Rxn. 3) could be fixed in the abiotic or biotic-abiotic coupling processes. In Fig. 8e, the experimental data for Fe(II) oxidation and NO_2^- reduction in the chemical treatment (Fe(II) + NO_2^-) were simulated with the result

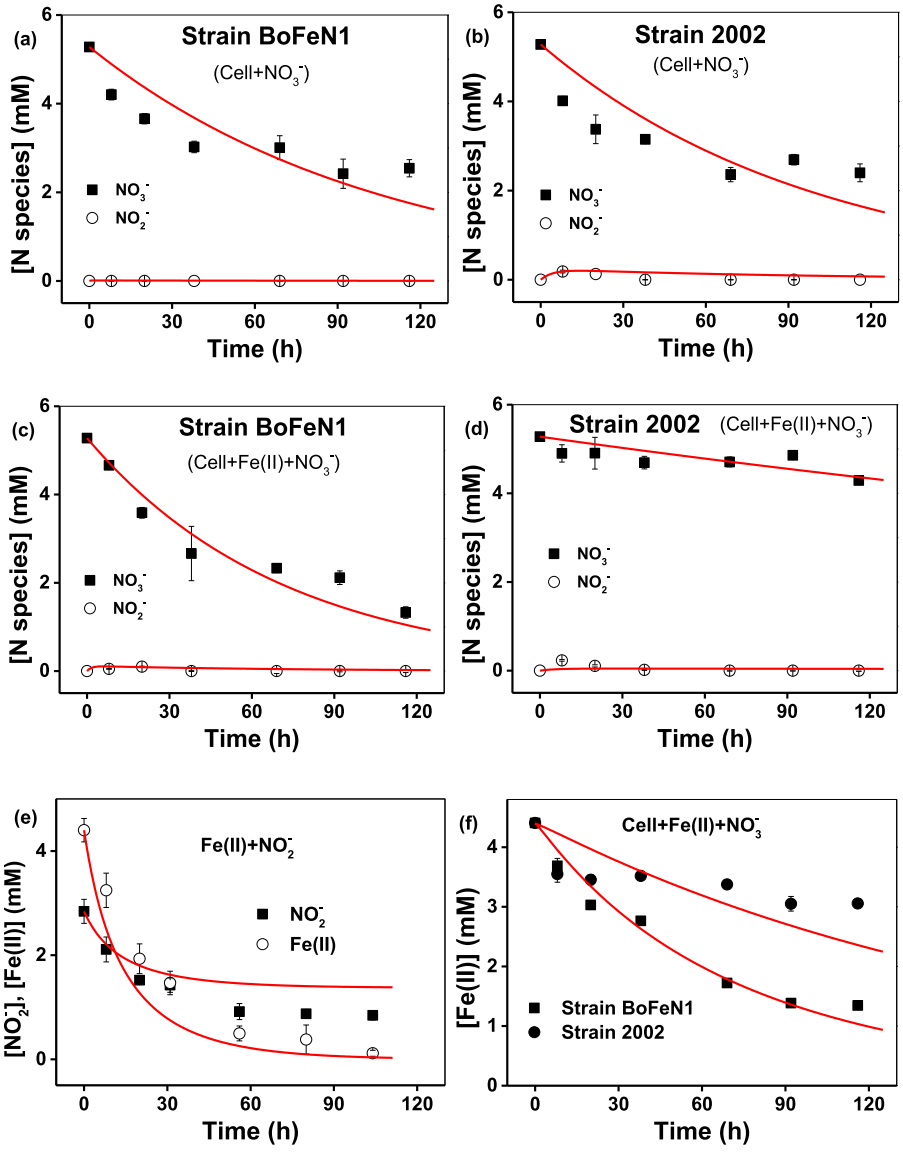

Fig. 8. Kinetics of NO_3^- reduction and NO_2^- formation for the different treatments with nitrate and/or Fe(II). (a) Strain BoFeN1 (Cells + NO_3^-); (b) Strain 2002 (Cells + NO_3^-); (c) Strain BoFeN1 (Cells + Fe(II) + NO_3^-); (d) Strain 2002 (Cells + Fe(II) + NO_3^-). The kinetics of Fe (II) oxidation and nitrite reduction for the different treatments with Fe(II). (e) Fe(II) + NO_2^-; (f) Cells + Fe(II) + NO_3^-. Red solid lines represent the model fit curves for Rxns. 1–4. Error bars represent the standard deviation of the mean (n = 3). (For interpretation of the references to colour in this figure legend, the reader is referred to the web version of this article.)

that the fitting curves for Fe(II) and NO_2^- were matched with the experimental data, and the optimal second-order rate constant (k_{chem}) was 2.63×10^{-3} M^{-1} s^{-1} (Table 3). The biological treatment (Cells + NO_3^-) was expressed according to Rxns. 1–4, so the kinetic model of the biological reduction of nitrate to nitrite and then to N_2O/N_2 could be established. From the fitting curves in Fig. 8a and b, the rate constants for nitrate reduction to nitrite ($k_{bio,1}$) and nitrite to N_2O/N_2 ($k_{bio,2}$) were obtained (Table 3). For the two strains (BoFeN1 and 2002), whereas their $k_{bio,1}$ values were very similar, the $k_{bio,2}$ for strain BoFeN1 was more than 19 times that for strain 2002. For strain 2002, the toxic effect might be attributed to the coverage of Fe(III) precipitation and the following cell encrustation from Fe(II) oxidation. However, it was found that strain BoFeN1 could secrete EPSs to protect the cell surface from encrustation (Klueglein et al., 2014), so this may be one of the reasons why Fe(II) oxidation did not cause obvious toxic effect on strain BoFeN1 (Carlson et al., 2012). In the treatment of Cells + Fe(II) + NO_3^-, the elementary reactions included all the reactions (Rxns. 1–4), hence the kinetic model for the nitrate reduction in the treatment of Cells + Fe(II) + NO_3^- was established. Both the values of $k_{bio,1}$ and $k_{bio,2}$ changed to different extents as compared with that for the biological treatment (Cells + NO_3^-). For the treatment of Cells + Fe(II) + NO_3^-, whereas the $k_{bio,1}$ for strain BoFeN1

Please cite this article in press as: Liu T., et al. Microbially mediated nitrate-reducing Fe(II) oxidation: Quantification of chemodenitrification and biological reactions. *Geochim. Cosmochim. Acta* (2018), https://doi.org/10.1016/j.gca.2018.06.040

Table 3
Model-derived rate constants of nitrate reduction and Fe(II) oxidation for the biological treatments with strains BoFeN1 and 2002 and the chemical treatment with Fe(II) and nitrite.

	Strain	k	Cells + NO_3^-	Cells + NO_3^-+Fe(II)	NO_2^-+Fe(II)	
Nitrate reduction	BoFeN1	$k_{bio,1}$ (s^{-1})	2.63×10^{-6}	3.87×10^{-6}	k_{chem} (M^{-1} s^{-1})	2.63×10^{-3}
		$k_{bio,2}$ (s^{-1})	1.22×10^{-3}	1.25×10^{-4}		
	2002	$k_{bio,1}$ (s^{-1})	2.78×10^{-6}	4.55×10^{-7}		
		$k_{bio,2}$ (s^{-1})	6.31×10^{-5}	4.42×10^{-5}		
Fe(II) oxidation	BoFeN1	$K_{bio,3}$ (s^{-1})	/	2.86×10^{-6}		
	2002	$K_{bio,3}$ (s^{-1})	/	1.18×10^{-7}		

only increased slightly, from 2.63×10^{-6} s^{-1} to 3.87×10^{-6} s^{-1} (Table 3), the $k_{bio,2}$ decreased substantially to 10% of $k_{bio,1}$. For strain 2002, both the values of $k_{bio,1}$ decreased dramatically, whereas $k_{bio,2}$ only slightly decreased, from 6.31×10^{-5} s^{-1} to 4.42×10^{-5} s^{-1}. Therefore, the nitrate/nitrite reduction capabilities of the two strains showed a very large discrepancy. Because both the strains and Fe(II) could reduce nitrite, the competition between biological nitrite reduction and chemodenitrification occurred in the treatment of Cells + Fe(II) + NO_3^-. When Fe(II) was fixed at 5 mM, the k_{chem} for NO_2^- was calculated as 1.32×10^{-5} s^{-1}, which was lower than that of $k_{bio,2}$ for strain BoFeN1 (1.25×10^{-4} s^{-1}) and for strain 2002 (4.42×10^{-5} s^{-1}), implying that the relative contribution of biological processes to the nitrite reduction was higher than that of chemodenitrification in the treatment of Cells + Fe(II) + NO_3^-. In addition, for Fe(II) oxidation, the kinetic model was also established according to the enzymatic and chemical Fe(II) oxidation via Rxns. 1–4. From Table 3 and the fitting curves in Fig. 8f, the $k_{bio,3}$ values were calculated as 2.86×10^{-6} s^{-1} for strain BoFeN1 and 1.18×10^{-7} s^{-1} for strain 2002. When NO_2^- was fixed at 2 mM, the k_{chem} for Fe(II) was calculated as 5.26×10^{-6} s^{-1}, which was higher than the $k_{bio,3}$ values for strains BoFeN1 and 2002, implying that the relative contribution of the chemical process by nitrite to the Fe(II) oxidation was higher than that of biological processes in the treatment of Cells + Fe(II) + NO_3^-.

To quantify the relative contributions of chemodenitrification and biological processes, the kinetic equations (Eqs. 1–4) for nitrite reduction and Fe(II) oxidation were combined. Based on the observed rate constants ($k_{bio,1}$, k_{chem}, and $k_{bio,3}$), and the model-derived concentrations of Fe(II) and nitrite, the relative contributions of biological reactions and chemodenitrification to Fe(II) oxidation and nitrite reduction could be eventually calculated from Eqs. 5–8.

$$Biotic\%(Fe(II)) = \frac{k_{bio,3}}{k_{bio,3} + k_{chem}[NO_2^-]} \quad \text{(Eq. 5)}$$

$$Abiotic\%(Fe(II)) = \frac{k_{chem}[NO_2^-]}{k_{bio,3} + k_{chem}[NO_2^-]} \quad \text{(Eq. 6)}$$

$$Biotic\%(NO_2^-) = \frac{k_{bio,2}}{k_{bio,2} + k_{chem}[Fe(II)]} \quad \text{(Eq. 7)}$$

$$Abiotic\%(NO_2^-) = \frac{k_{chem}[Fe(II)]}{k_{bio,2} + k_{chem}[Fe(II)]} \quad \text{(Eq. 8)}$$

The results in Fig. 9 clearly showed the relative proportion of biological reactions and chemodenitrification to Fe(II) oxidation and nitrite reduction. The model indicated that the relative contribution of chemodenitrification to nitrite reduction was different from that to Fe(II) oxidation. To nitrite reduction, biological processes played a more important role than chemodenitrification did, whereas to Fe(II) oxidation, the relative contribution of chemodenitrification was higher than that of the biological processes.

4.4. Methodological significance and environmental implications

So far, less direct observation has been reported to prove the existence of enzymatic Fe(II)-oxidation by microorganisms, and details of the chemical process of Fe(II) oxidation at a molecular scale are still lacking. In the microbe-Fe(II)-nitrate complex system, there are many challenges to evaluate the integration of the biological and chemical processes. Proteomic and molecular biological techniques can be used to identify the key Fe(II) oxidase and electron transfer chains in the microbe-Fe(II)-nitrate system (He et al., 2016, 2017). Whereas some candidate functional proteins (i.e., *c*-Cyts) might specifically account for the Fe(II) oxidation, direct kinetic information concerning their enzymatic Fe(II) oxidation capability has not been produced in detail. For iron-oxidizing bacteria, despite the progress in the *in vitro* studies on *c*-Cyts and Fe(II), it would be promising to directly investigate *in vivo* Fe(II)-oxidizing proteins and Fe(II) using the *in situ* spectral method, or extract the EPSs containing c-Cyts for *in vitro* kinetic studies. Fortunately, the *in situ* spectroscopy has been used to directly measure reaction kinetics between Fe(II) and *c*-Cyts in both living cells and EPSs of the two Fe(II)-oxidizing strains, which would show the theoretical capability of taking electrons from Fe(II) into the cells.

Distinguishing the relative contributions of abiotic and enzymatically catalyzed reactions remains a big challenge (Melton et al., 2014). Whereas the contribution of biotic processes apparently can be determined by using traditional control experiments, the co-occurrence of biotic and abiotic reactions is hardly addressed. This co-occurrence is essential to facilitating the estimation of the contribution of both chemical and microbial reactions and to providing insights into their interactions. Iron and nitrogen stable isotope fractionation is considered a potential technology for distinguishing and quantifying the biological and chemical

Please cite this article in press as: Liu T., et al. Microbially mediated nitrate-reducing Fe(II) oxidation: Quantification of chemodenitrification and biological reactions. *Geochim. Cosmochim. Acta* (2018), https://doi.org/10.1016/j.gca.2018.06.040

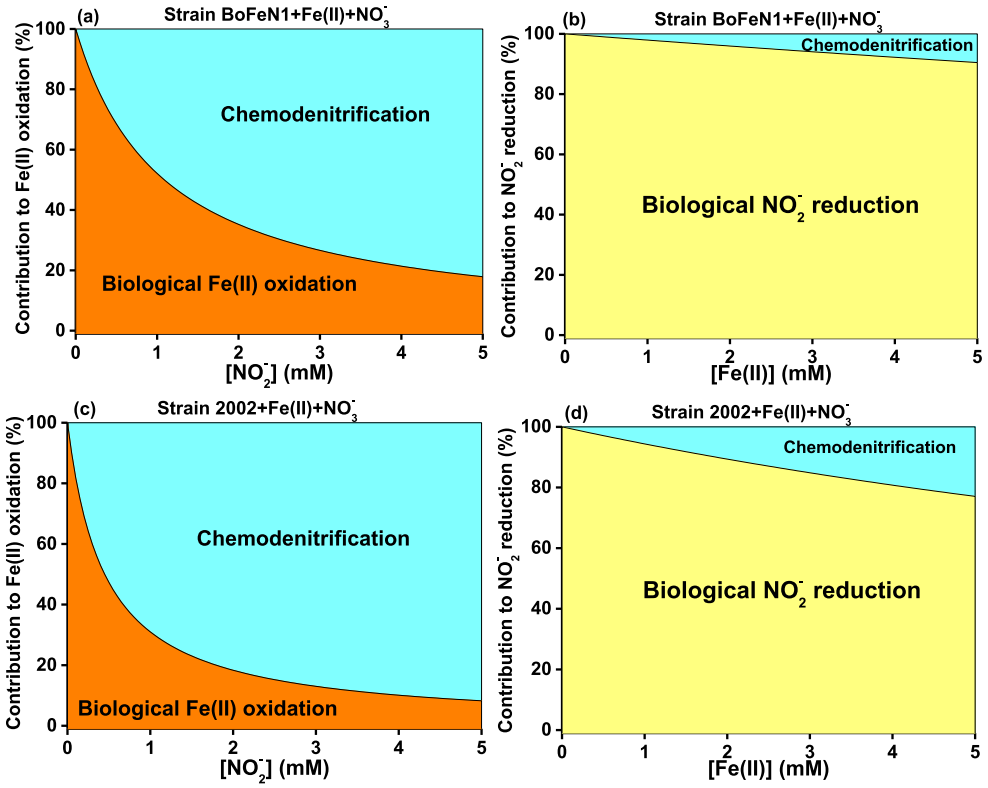

Fig. 9. The relative contribution of biological and chemodenitrification to Fe(II) oxidation as a function of nitrite concentration and nitrite reduction as a function of Fe(II) concentration. (a) and (c) represented the relative contribution of chemical Fe(II) oxidation by NO_2^- (chemodenitrification) and the potential biological Fe(II) oxidation; (b) and (d) represented the relative contribution of chemical NO_2^- reduction by Fe(II) (chemodenitrification) and biological NO_2^- reduction by two strains with acetate as electron donors.

reactions (Cooper et al., 2003; Kappler et al., 2010), which was attempted in our recent research (Chen et al., 2018). Besides the direct experimental approach, the elementary-reaction-based kinetic modeling approaches might be ideal for quantitatively evaluating the contributions of the biological and chemical processes involved in microbially mediated NO_3^--reducing Fe(II) oxidation. Based on the separate confirmation of chemodenitrification and biological reactions, the model for the whole microbially mediated NRFO could be established according to their detailed elementary reactions. From the obtained rate constants of both abiotic and biotic reactions for NO_3^- reduction and Fe(II) oxidation, the relative contributions of chemical and biological processes to Fe and N transformation could be quantitatively evaluated. It is clearly seen that the biological nitrate reduction played a key role in nitrate/nitrite reduction, whereas the chemodenitrification process acted as the dominant driving force for Fe(II) oxidation. Since the model established could provide a quantitative picture of the biological and chemical processes for the NRFO system, such a simple model might have a potential to be applied to other analogous systems which also include the coupling biological–chemical processes. A quantitative analysis of the biological and chemical processes based on the model would be used for predicating the relative contributions of each process under any conditions with different species and concentrations, so it can certainly improve the understanding of the complicated natural processes.

These findings may have implications for providing even broader perspective for disentangling the molecular-scale mechanisms of microbially mediated NO_3^--reducing Fe(II) oxidation processes and may be helpful for understanding NRFO-related issues, such as Fe mineralization and greenhouse gas N_2O emissions. In previous studies of microbially mediated NO_3^--reducing Fe(II) oxidation, biological Fe(II) oxidation was usually overestimated, whereas the chemical Fe(II) oxidation by nitrite was largely overlooked, and hence, the NRFO system needs an updated interpretation to understand the underlying mechanisms (Klueglein and Kappler, 2013). Identification and quantification of N_2O sinks on the Earth's surface is an important part of improving the global N_2O budget (Doane, 2017). Although biological and abiotic N_2O production has been widely documented, the environmental roles of such remain unclear (Zhu-Barker et al., 2015). In the current study, whereas no significant amount of N_2O was observed in the treatment of Cells + NO_3^-, N_2O was steadily generated during the chemical reaction between Fe(II) and NO_2^-, and N_2O production was also observed after the addition of Fe(II) in the Cells + NO_3^- treatment for both strain BoFeN1 and strain 2002. Hence, the presence of Fe(II) in similar environments may elevate N_2O emissions. It was reported that high

Please cite this article in press as: Liu T., et al. Microbially mediated nitrate-reducing Fe(II) oxidation: Quantification of chemodenitrification and biological reactions. *Geochim. Cosmochim. Acta* (2018), https://doi.org/10.1016/j.gca.2018.06.040

levels of Fe(II) had been shown to increase N_2O yield (Buchwald et al., 2016; Grabb et al., 2017), and chemodenitrification reaction rates were also promoted by elevated levels of Fe(II) (Heil et al., 2015; Jones et al., 2015; Peters et al., 2014). The positive flux of NO_2^- together with the porewater Fe(II) levels suggests that chemodenitrification may also have contributed to N_2O production (Michiels et al., 2017; Wankel et al., 2017). The study also implied that the nitrate/nitrite disappearance in some specific environments (i.e., flooded paddy soils and sediments) might be obviously determined by the concentrations of Fe(II) which could be generated from the microbial iron reduction.

5. CONCLUSIONS

Our results demonstrated that the effect of Fe(II) on microbial NO_3^- reduction was different between the strains 2002 and BoFeN1, in which Fe(II) slightly accelerated the NO_3^- reduction by strain BoFeN1, but substantially retarded that by strain 2002. The Fe(II) oxidation was accompanied by microbial NO_3^- reduction and resulted in the formation of secondary minerals (i.e. lepidocrocite, goethite, and magnetite), which was also different from that (only goethite) in chemodenitrification. The *c*-Cyts in the EPSs was reduced by Fe(II), which suggest *c*-Cyts in the EPSs has the theoretical capability of taking electrons from Fe(II) into the cells. Based on the kinetics data of microbial NO_3^-/NO_2^- reduction and chemodenitrification, the brief model established in this study not only enable us to obtain the rate constant of Fe(II) oxidation by *c*-Cyts in the EPSs, but also provide the information about the relative contribution of each process to nitrite reduction and Fe(II) oxidation. Though the chemodenitrification revealed a relatively higher reaction rate than the microbial reaction system, our model indicated that the relative contribution of chemodenitrification to nitrite reduction is different from that to Fe(II) oxidation. To nitrite reduction, biological processes played a more important role than chemodenitrification did, whereas to Fe(II) oxidation, the relative contribution of chemodenitrification was higher than that of the biological processes. The findings provide new insight into the relative importance of chemodenitrification and biological reactions in microbially mediated nitrate-reducing Fe(II) oxidation, and improve our understanding of the biogeochemical cycles of iron and nitrogen in subsurface environments.

ACKNOWLEDGEMENTS

This work was funded by the National Natural Science Foundation of China (41571130052 and 41522105), Local Innovative and Research Teams Project of Guangdong Pearl River Talents Program (2017BT01Z176), Guangdong Natural Science Fund for Distinguished Young Scholars (2017A030306010), Excellent Talent Fund of Guangdong Academy of Sciences in China (2017GDASCX-0408), and SPICC program of GDAS (Scientific Platform and Innovation Capability Construction). We are grateful for the help for the $\delta^{15}N$ and N_2 concentration test from Institute of Urban Environment, Chinese Academy of Sciences, China. We sincerely thank Prof. Andreas Kappler at University of Tübingen for kindly providing the bacterium *Acidovorax* sp. strain BoFeN1. We also sincerely appreciate three anonymous reviewers for their very constructive comments and suggestions.

REFERENCES

Beller H. R., Peng Z., Legler T. C., Chakicherla A., Kane S., Letain T. E. and O'Day P. A. (2013) Genome-enabled studies of anaerobic, nitrate-dependent iron oxidation in the chemolithoautotrophic bacterium *Thiobacillus denitrificans*. *Front. Microbiol.* **4**, 249–265.

Benz M., Brune A. and Schink B. (1998) Anaerobic and aerobic oxidation of ferrous iron at neutral pH by chemoheterotrophic nitrate-reducing bacteria. *Arch. Microbiol.* **169**, 159–165.

Bird L. J., Bonnefoy V. and Newman D. K. (2011) Bioenergetic challenges of microbial iron metabolisms. *Trends microbiol.* **19**, 330–340.

Blöthe M. and Roden E. E. (2009) Composition and activity of an autotrophic Fe(II)-oxidizing, nitrate-reducing enrichment culture. *Appl. Environ. Microbiol.* **75**, 6937–6940.

Blake, II, R. C., Anthony M. D., Bates J. D., Hudson T., Hunter K. M., King B. J., Landry B. L., Lewis M. L. and Painter R. G. (2016) *In situ* spectroscopy reveals that microorganisms in different phyla use different electron transfer biomolecules to respire aerobically on soluble iron. *Front. Microbiol.* **7**, 1963–1972.

Blake, II, R. C. and Griff M. N. (2012) *In situ* spectroscopy on intact *Leptospirillum ferrooxidans* reveals that reduced cytochrome 579 is an obligatory intermediate in the aerobic iron respiratory chain. *Front. Microbiol.* **3**, 136–146.

Borch T., Kretzschmar R., Kappler A., Cappellen P. V., Ginder-Vogel M., Voegelin A. and Campbell K. (2010) Biogeochemical redox processes and their impact on contaminant dynamics. *Environ. Sci. Technol.* **44**, 15–23.

Buchwald C., Grabb K., Hansel C. M. and Wankel S. D. (2016) Constraining the role of iron in environmental nitrogen transformations: dual stable isotope systematics of abiotic NO_2^- reduction by Fe(II) and its production of N_2O. *Geochim. Cosmochim. Acta* **186**, 1–12.

Cao B., Ahmed B., Kennedy D., Wang Z., Shi L., Marshall M., Fredrickson J., Isern N., Majors P. and Beyenal H. (2011) Contribution of extracellular polymeric substances from *Shewanella* sp. HRCR-1 biofilms to U(VI) immobilization. *Environ. Sci. Technol.* **45**, 5483–5490.

Carlson H. K., Clark I. C., Blazewicz S. J., Iavarone A. T. and Coates J. D. (2013) Fe(II) oxidation is an innate capability of nitrate-reducing bacteria that involves abiotic and biotic reactions. *J. Bacteriol.* **195**, 3260–3268.

Carlson H. K., Clark I. C., Melnyk R. A. and Coates J. D. (2012) Toward a mechanistic understanding of anaerobic nitrate-dependent iron oxidation: balancing electron uptake and detoxification. *Front. Microbiol.* **3**, 57–62.

Chen D., Liu T., Li X., Li F., Luo X., Wu Y. and Wang Y. (2018) Biological and chemical processes of microbially mediated nitrate-reducing Fe(II) oxidation by *Pseudogulbenkiania* sp. strain 2002. *Chem. Geol.* **476**, 59–69.

Coby A. J. and Picardal F. W. (2005) Inhibition of NO_3^- and NO_2^- reduction by microbial Fe(III) reduction: evidence of a reaction between NO_2^- and cell surface-bound Fe^{2+}. *Appl. Environ. Microbiol.* **71**, 5267–5274.

Cooper D. C., Picardal F. W., Schimmelmann A. and Coby A. J. (2003) Chemical and biological interactions during nitrate and goethite reduction by *Shewanella putrefaciens* 200. *Appl. Environ. Microbiol.* **69**, 3517–3525.

Croal L. R., Gralnick J. A., Malasarn D. and Newman D. K. (2004) The genetics of geochemistry. *Annu. Rev. Genet.* **38**, 175–202.

David E., Field E. K., Olga C., Davenport K. W., Lynne G., Christine M., Matt N. and Tanja W. (2013) Comparative genomics of freshwater Fe-oxidizing bacteria: implications for physiology, ecology, and systematics. *Front. Microbiol.* **4**, 254–271.

Ding L., An X., Li S., Zhang G. and Zhu Y. (2014) Nitrogen loss through anaerobic ammonium oxidation coupled to iron reduction from paddy soils in a chronosequence. *Environ. Sci. Technol.* **48**, 10641–10647.

Doane T. A. (2017) The abiotic nitrogen cycle. *ACS Earth Space Chem.* **1**, 411–421.

Emerson D., Fleming E. J. and McBeth J. M. (2010) Iron-oxidizing bacteria: an environmental and genomic perspective. *Annu. Rev. Microbiol.* **64**, 561–583.

Etique M., Jorand F. P., Zegeye A., Grégoire B., Despas C. and Ruby C. (2014) Abiotic process for Fe(II) oxidation and green rust mineralization driven by a heterotrophic nitrate reducing bacteria (*Klebsiella mobilis*). *Environ. Sci. Technol.* **48**, 3742–3751.

Grabb K. C., Buchwald C., Hansel C. and Wankel S. D. (2017) A dual nitrite isotopic investigation of chemodenitrification by mineral-associated Fe(II) and its production of nitrous oxide. *Geochim. Cosmochim. Acta* **196**, 388–402.

Hafenbradl D., Keller M., Dirmeier R., Rachel R., Rossnagel P., Burggraf S., Huber H. and Stetter K. O. (1996) *Ferroglobus placidus* gen nov, sp nov, a novel hyperthermophilic archaeum that oxidizes Fe^{2+} at neutral pH under anoxic conditions. *Arch. Microbiol.* **166**, 308–314.

Han R., Li F., Liu T., Li X., Wu Y., Wang Y. and Chen D. (2016) Effects of incubation conditions on Cr(VI) reduction by *c*-type cytochromes in intact *Shewanella oneidensis* MR-1 cells. *Front. Microbiol.* **7**, 746–758.

Han R., Li X., Wu Y., Li F. and Liu T. (2017) *In situ* spectral kinetics of quinone reduction by *c*-type cytochromes in intact *Shewanella oneidensis* MR-1 cells. *Colloids Surf. A* **520**, 505–513.

Hansen H. C. B., Guldberg S., Erbs M. and Koch C. B. (2001) Kinetics of nitrate reduction by green rusts—effects of interlayer anion and Fe(II):Fe(III) ratio. *Appl. Clay Sci.* **18**, 81–91.

Hansen H. C. B., Koch C. B., Krogh H. N., Borggaard O. and SØrensen J. (1996) Abiotic nitrate reduction to ammonium: key role of green rust. *Environ. Sci. Technol.* **30**, 2053–2056.

He S., Barco R. A., Emerson D. and Roden E. E. (2017) Comparative genomic analysis of neutrophilic Iron(II) oxidizer genomes for candidate genes in extracellular electron transfer. *Front. Microbiol.* **8**, 1584–1601.

He S., Tominski C., Kappler A., Behrens S. and Roden E. E. (2016) Metagenomic analyses of the autotrophic Fe(II)-oxidizing, nitrate-reducing enrichment Culture KS. *Appl. Environ. Microbiol.* **82**, 2656–2668.

Hedrich S., Schlomann M. and Johnson D. B. (2011) The iron-oxidizing proteobacteria. *Microbiol.* **157**, 1551–1564.

Heil J., Liu S., Vereecken H. and Brüggemann N. (2015) Abiotic nitrous oxide production from hydroxylamine in soils and their dependence on soil properties. *Soil Biol. Biochem.* **84**, 107–115.

Ilbert M. and Bonnefoy V. (2013) Insight into the evolution of the iron oxidation pathways. *Biochim. Biophys. Acta* **1827**, 161–175.

Ishii S., Joikai K., Otsuka S., Senoo K. and Okabe S. (2016) Denitrification and nitrate-dependent Fe(II) oxidation in various *Pseudogulbenkiania* strains. *Microbes Environ.* **31**, 293–298.

Johnson K., Simpson Z. and Blom T. (2009) Global kinetic explorer: a new computer program for dynamic simulation and fitting of kinetic data. *Anal. Biochem.* **387**, 20–29.

Jones L. C., Brian P., Pacheco J. S., Lezama Casciotti K. L. and Scott F. (2015) Stable isotopes and iron oxide mineral products as markers of chemodenitrification. *Environ. Sci. Technol.* **49**, 3444–3452.

Kampschreur M. J., Kleerebezem R., De Vet W. W. and Van Loosdrecht M. C. (2011) Reduced iron induced nitric oxide and nitrous oxide emission. *Water Res.* **45**, 5945–5952.

Kappler A., Johnson C. M., Crosby H. A., Beard B. L. and Newman D. K. (2010) Evidence for equilibrium iron isotope fractionation by nitrate-reducing iron(II)-oxidizing bacteria. *Geochim. Cosmochim. Acta* **74**, 2826–2842.

Kappler A., Schink B. and Newman D. K. (2005) Fe(III) mineral formation and cell encrustation by the nitrate-dependent Fe(II)-oxidizer strain BoFeN1. *Geobiology* **3**, 235–245.

Kappler A. and Straub K. L. (2005) Geomicrobiological cycling of iron. *Rev. Mineral. Geochem.* **59**, 85–108.

Klueglein N. and Kappler A. (2013) Abiotic oxidation of Fe(II) by reactive nitrogen species in cultures of the nitrate-reducing Fe (II) oxidizer *Acidovorax* sp. BoFeN1 - questioning the existence of enzymatic Fe(II) oxidation. *Geobiology* **11**, 180–190.

Klueglein N., Picardal F., Zedda M., Zwiener C. and Kappler A. (2015) Oxidation of Fe(II)-EDTA by nitrite and by two nitrate-reducing Fe(II)-oxidizing *Acidovorax* strains. *Geobiology* **13**, 198–207.

Klueglein N., Zeitvogel F., Stierhof Y.-D., Floetenmeyer M., Konhauser K. O., Kappler A. and Obst M. (2014) Potential role of nitrite for abiotic Fe(II) oxidation and cell encrustation during nitrate reduction by denitrifying bacteria. *Appl. Environ. Microbiol.* **80**, 1051–1061.

Konhauser K. O., Kappler A. and Roden E. E. (2011) Iron in microbial metabolisms. *Elements* **7**, 89–93.

Kopf S. H., Henny C. and Newman D. K. (2013) Ligand-enhanced abiotic iron oxidation and the effects of chemical versus biological iron cycling in anoxic environments. *Environ. Sci. Technol.* **47**, 2602–2611.

Kumaraswamy R., Sjollema K., Kuenen G., van Loosdrecht M. and Muyzer G. (2006) Nitrate-dependent $[Fe(II)EDTA]^{2-}$ oxidation by *Paracoccus ferrooxidans* sp. nov., isolated from a denitrifying bioreactor. *Syst. Appl. Microbiol.* **29**, 276–286.

Kustin K., Taub I. A. and Weinstock E. (1966) A kinetic study of the formation of the ferrous-nitric oxide complex. *Inorg. Chem.* **5**, 1079–1082.

Laufer K., Røy H., Jørgensen B. B. and Kappler A. (2016) Evidence for the existence of autotrophic nitrate-reducing Fe (II)-oxidizing bacteria in marine coastal sediment. *Appl. Microbiol. Biotechnol.* **82**, 6120–6131.

Lewicka-Szczebak D., Well R., Giesemann A., Rohe L. and Wolf U. (2013) An enhanced technique for automated determination of ^{15}N signatures of N_2, (N_2 +N_2O) and N_2O in gas samples. *Rapid Commun. Mass Spectrom.* **27**, 1548–1558.

Li B., Deng C., Zhang D., Pan X., Al-misned F. A. and Mortuza M. G. (2016a) Bioremediation of nitrate-and arsenic-contaminated groundwater using nitrate-dependent Fe(II) oxidizing *Clostridium* sp strain pxl2. *Geomicrobiol. J.* **33**, 185–193.

Li X., Hou L., Liu M., Zheng Y., Yin G., Lin X., Cheng L., Li Y. and Hu X. (2015) Evidence of nitrogen loss from anaerobic ammonium oxidation coupled with ferric iron reduction in an intertidal wetland. *Environ. Sci. Technol.* **49**, 11560–11568.

Li X., Zhang W., Liu T., Chen L., Chen P. and Li F. (2016b) Changes in the composition and diversity of microbial communities during anaerobic nitrate reduction and Fe(II) oxidation at circumneutral pH in paddy soil. *Soil Biol. Biochem.* **94**, 70–79.

Li X., Zhou S., Li F., Wu C., Zhuang L., Xu W. and Liu L. (2009) Fe(III) oxide reduction and carbon tetrachloride dechlorination by a newly isolated *Klebsiella pneumoniae* strain L17. *J. Appl. Microbiol.* **106**, 130–139.

Please cite this article in press as: Liu T., et al. Microbially mediated nitrate-reducing Fe(II) oxidation: Quantification of chemodenitrification and biological reactions. *Geochim. Cosmochim. Acta* (2018), https://doi.org/10.1016/j.gca.2018.06.040

Li Y., Yu S., Strong J. and Wang H. (2012) Are the biogeochemical cycles of carbon, nitrogen, sulfur, and phosphorus driven by the "Fe^{III}-Fe^{II} redox wheel" in dynamic redox environments? *J. Soils Sediments* **12**, 683–693.

Liu J., Wang Z., Belchik S. M., Edwards M. J., Liu C., Kennedy D. W., Merkley E. D., Lipton M. S., Butt J. N., Richardson D. J., Zachara J. M., Fredrickson J. K., Rosso K. M. and Shi L. (2012) Identification and characterization of MtoA: a decaheme *c*-type cytochrome of the neutrophilic Fe(II)-oxidizing bacterium *Sideroxydans lithotrophicus* ES-1. *Front. Microbiol.* **3**, 37–48.

Liu T., Li X., Li F., Han R., Wu Y., Yuan X. and Wang Y. (2016) *In situ* spectral kinetics of Cr(VI) reduction by *c*-type cytochromes in a suspension of living *Shewanella putrefaciens* 200. *Sci. Rep.*, 6.

Liu T., Li X., Li F. and Zhang W. (2014a) Fe(III) oxides accelerate microbial nitrate reduction and electricity generation by *Klebsiella pneumoniae* L17. *J. Colloid Interface Sci.* **423**, 25–32.

Liu T., Li X., Li F. and Zhang W. (2014b) Kinetics of competitive reduction of nitrate and iron oxides by *Aeromonas hydrophila* HS01. *Soil Sci. Soc. Am. J.* **78**, 1903–1912.

Liu T., Wang Y., Li X. and Li F. (2017a) Redox dynamics and equilibria of *c*-type cytochromes in the presence of Fe(II) under anoxic conditions: insights into enzymatic iron oxidation. *Chem. Geol.* **468**, 97–104.

Liu T., Wu Y., Li F., Li X. and Luo X. (2017b) Rapid redox processes of *c*-type cytochromes in a living cell suspension of *Shewanella oneidensis* MR-1. *Chemistryselect* **2**, 1008–1012.

Luo X., Wu Y., Li X., Chen D., Wang Y., Li F. and Liu T. (2017) The *in situ* spectral methods for examining redox status of *c*-type cytochromes in metal-reducing/oxidizing bacteria. *Acta Geochim.* **36**, 544–547.

Matsuno T., Mie Y., Yoshimune K. and Yumoto I. (2009) Physiological role and redox properties of a small cytochrome c (5), cytochrome c-552, from alkaliphile, P*seudomonas alcaliphila* AL15-21(T). *J. Biosci. Bioeng.* **108**, 465–470.

Melton E. D., Swanner E. D., Behrens S., Schmidt C. and Kappler A. (2014) The interplay of microbially mediated and abiotic reactions in the biogeochemical Fe cycle. *Nat. Rev. Microbiol.* **12**, 797–808.

Michiels C. C., Darchambeau F., Roland F. A. E., Morana C., Llirós M., Garcíaarmisen T., Bo T., Borges A. V., Canfield D. E. and Servais P. (2017) Iron-dependent nitrogen cycling in a ferruginous lake and the nutrient status of Proterozoic oceans. *Nat. Geosci.*, 10.

Miot J., Benzerara K., Morin G., Bernard S., Beyssac O., Larquet E., Kappler A. and Guyot F. (2009a) Transformation of vivianite by anaerobic nitrate-reducing iron-oxidizing bacteria. *Geobiology* **7**, 373.

Miot J., Benzerara K., Morin G., Kappler A., Bernard S., Obst M., Férard C., Skouripanet F., Guigner J. M. and Posth N. (2009b) Iron biomineralization by anaerobic neutrophilic iron-oxidizing bacteria. *Geochim. Cosmochim. Acta* **73**, 696–711.

Miot J., Li J., Benzerara K., Sougrati M. T., Ona-Nguema G., Bernard S., Jumas J. C. and Guyot F. (2014) Formation of single domain magnetite by green rust oxidation promoted by microbial anaerobic nitrate-dependent iron oxidation. *Geochim. Cosmochim. Acta* **139**, 327–343.

Moraghan J. T. and Buresh R. J. (1976) Chemical reduction of nitrite and nitrous oxide by ferrous iron. *Soil Sci. Soc. Am. J.* **41**, 47–50.

Mulvaney R. (1984) Determination of ^{15}N-labeled dinitrogen and nitrous oxide with triple-collector mass spectrometers. *Soil Sci. Soc. Am. J.* **48**, 690–692.

Nakamura R., Ishii K. and Hashimoto K. (2009) Electronic absorption spectra and redox properties of *c*-type cytochromes in living microbes. *Angew. Chem. Int. Ed.* **48**, 1606–1608.

Neubauer S. C., Emerson D. and Megonigal J. P. (2002) Life at the energetic rdge: kinetics of circumneutral iron oxidation by lithotrophic iron-oxidizing bacteria isolated from the wetland-plant rhizosphere. *Appl. Environ. Microbiol.* **68**, 3988–3995.

Nordhoff M., Tominski C., Halama M., Byrne J. M., Obst M., Kleindienst S., Behrens S. and Kappler A. (2017) Insights into nitrate-reducing Fe(II) oxidation mechanisms through analysis of cell-mineral associations, cell encrustation, and mineralogy in the chemolithoautotrophic enrichment culture KS. *Appl. Environ. Microbiol.*, 83.

Ottley C. J., Davison W. and Edmunds W. M. (1997) Chemical catalysis of nitrate reduction by iron(II). *Geochim. Cosmochim. Acta* **61**, 1819–1828.

Pantke C., Obst M., Benzerara K., Morin G., Onanguema G., Dippon U. and Kappler A. (2012) Green rust formation during Fe(II) oxidation by the nitrate-reducing *Acidovorax* sp. strain BoFeN1. *Environ. Sci. Technol.* **46**, 1439–1446.

Pearsall K. A. and Bonner F. T. (1982) Aqueous nitrosyliron(II) chemistry. 2. Kinetics and mechanism of nitric-oxide reduction–the dinitrosyl complex. *Inorg. Chem.* **21**, 1978–1985.

Peters B., Casciotti K. L., Samarkin V. A., Madigan M. T., Schutte C. A. and Joye S. B. (2014) Stable isotope analyses of NO_2^-, NO_3^-, and N_2O in the hypersaline ponds and soils of the McMurdo Dry Valleys, Antarctica. *Geochim. Cosmochim. Acta* **135**, 87–101.

Pham A. N. and Waite T. D. (2008) Modeling the kinetics of Fe(II) oxidation in the presence of citrate and salicylate in aqueous solutions at pH 6.0-8.0 and 25 °C. *J. Phys. Chem. A* **112**, 5395–5405.

Picardal F. (2012) Abiotic and microbial interactions during anaerobic transformations of Fe(II) and NO_x. *Front. Microbiol.* **3**, 112–118.

Rakshit S., Matocha C. J. and Coyne M. S. (2008) Nitrite reduction by siderite. *Soil Sci. Soc. Am. J.* **72**, 1070–1077.

Rakshit S., Matocha C. J., Coyne M. S. and Sarkar D. (2016) Nitrite reduction by Fe(II) associated with kaolinite. *Int. J. Environ. Sci. Technol.* **13**, 1329–1334.

Rancourt D. G., Thibault P. J., Mavrocordatos D. and Lamarche G. (2005) Hydrous ferric oxide precipitation in the presence of nonmetabolizing bacteria: constraints on the mechanism of a biotic effect. *Geochim. Cosmochim. Acta* **69**, 553–577.

Ratering S. and Schnell S. (2001) Nitrate-dependent iron(II) oxidation in paddy soil. *Environ. Microbiol.* **3**, 100–109.

Rentz J. A., Kraiya C., Luther G. W. and Emerson D. (2007) Control of ferrous iron oxidation within circumneutral microbial iron mats by cellular activity and autocatalysis. *Environ. Sci. Technol.* **41**, 6084–6089.

Roden E. E. (2012) Microbial iron-redox cycling in subsurface environments. *Biochem. Soc. Trans.* **40**, 1249–1256.

Schaedler F., Lockwood C., Lueder U., Glombitza C., Kappler A. and Schmidt C. (2017) Microbially mediated coupling of Fe and N cycles by nitrate-reducing Fe(II)-oxidizing bacteria in littoral freshwater sediments. *Appl. Environ. Microbiol.*.

Schädler S., Burkhardt C., Hegler F. and Straub K. L. (2009) Formation of cell-iron-mineral aggregates by phototrophic and nitrate-reducing anaerobic Fe(II)-oxidizing bacteria. *Geomicrobiol. J.* **26**, 93–103.

Schmid G., Zeitvogel F., Hao L., Ingino P., Flötenmeyer M., Stierhof Y. D., Schröppel B., Burkhardt C., Kappler A. and Obst M. (2014) 3-D analysis of bacterial cell-(iron) mineral aggregates formed during Fe(II) oxidation by the nitrate-reducing *Acidovorax sp.* strain BoFeN1 using complementary microscopy tomography approaches. *Geobiology* **12**, 340–361.

Shelobolina E., Konishi H., Xu H., Benzine J., Mai Y. X., Tao W., Blöthe M. and Roden E. (2012) Isolation of phyllosilicate–iron

Please cite this article in press as: Liu T., et al. Microbially mediated nitrate-reducing Fe(II) oxidation: Quantification of chemodenitrification and biological reactions. *Geochim. Cosmochim. Acta* (2018), https://doi.org/10.1016/j.gca.2018.06.040

redox cycling microorganisms from an illite–smectite rich hydromorphic soil. *Front. Microbiol.* **3**, 134–143.

Smith R. L., Kent D. B., Repert D. A. and Böhlke J. K. (2017) Anoxic nitrate reduction coupled with iron oxidation and attenuation of dissolved arsenic and phosphate in a sand and gravel aquifer. *Geochim. Cosmochim. Acta* **196**, 102–120.

Sorokina A. Y., Chernousova E. Y. and Dubinina G. A. (2012) *Hoeflea siderophila* sp. nov., a new neutrophilic iron-oxidizing bacterium. *Microbiol.* **81**, 59–66.

Straub K. L., Benz M. and Schink B. (2001) Iron metabolism in anoxic environment at near neutral pH. *FEMS Microbiol. Ecol.* **34**, 181–186.

Straub K. L., Benz M., Schink B. and Widdel F. (1996) Anaerobic, nitrate-dependent microbial oxidation of ferrous iron. *Appl. Environ. Microbiol.* **62**, 1458–1460.

Straub K. L., Schber W. A., Buchholz-Cleven B. E. E. and Schink B. (2004) Diversity of ferrous iron-oxidizing, nitrate-reducing bacteria and their involvement in oxygen-independent iron cycling. *Geomicrobiol. J.* **21**, 371–378.

Sun J., Chillrud S. N., Mailloux B. J., Stute M., Singh R., Dong H., Lepre C. J. and Bostick B. C. (2016) Enhanced and stabilized arsenic retention in microcosms through the microbial oxidation of ferrous iron by nitrate. *Chemosphere* **144**, 1106–1115.

Wankel S. D., Ziebis W., Buchwald C., Charoenpong C., De B. D., Dentinger J., Xu Z. and Zengler K. (2017) Evidence for fungal and chemodenitrification based N_2O flux from nitrogen impacted coastal sediments. *Nat. Commun.*, 8.

Weber K. A., Achenbach L. A. and Coates J. D. (2006a) Microorganisms pumping iron: anaerobic microbial iron oxidation and reduction. *Nat. Rev. Microbiol.* **4**, 752–764.

Weber K. A., Hedrick D. B., Peacock A. D., Thrash J. C., White D. C., Achenbach L. A. and Coates J. D. (2009) Physiological and taxonomic description of the novel autotrophic, metal oxidizing bacterium, *Pseudogulbenkiania* sp strain 2002. *Appl. Microbiol. Biotechnol.* **83**, 555–565.

Weber K. A., Pollock J., Cole K. A., O'Connor S. M., Achenbach L. A. and Coates J. D. (2006b) Anaerobic nitrate-dependent iron(II) bio-oxidation by a novel lithoautotrophic betaproteobacterium, strain 2002. *Appl. Environ. Microbiol.* **72**, 686–694.

Xi D., Ren B., Zhang L. and Fang Y. (2016) Contribution of anammox to nitrogen removal in two temperate forest soils. *Appl. Environ. Microbiol.* **82**, 4602–4612.

Xiu W., Guo H., Shen J., Liu S., Ding S., Hou W., Ma J. and Dong H. (2016) Stimulation of Fe(II) oxidation, biogenic lepidocrocite formation and arsenic immobilization by *Pseudogulbenkiania* sp. strain 2002. *Environ. Sci. Technol.* **50**, 6449–6458.

Zhang W., Liu T., Li X. and Li F. (2012) Enhanced nitrate reduction and current generation by *Bacillus* sp. in the presence of iron oxides. *J. Soils Sediments* **12**, 354–365.

Zhao L., Dong H., Edelmann R. E., Zeng Q. and Agrawal A. (2017) Coupling of Fe(II) oxidation in illite with nitrate reduction and its role in clay mineral transformation. *Geochim. Cosmochim. Acta* **200**, 353–366.

Zhao L., Dong H., Kukkadapu R., Agrawal A., Liu D., Zhang J. and Edelmann R. E. (2013) Biological oxidation of Fe(II) in reduced nontronite coupled with nitrate reduction by *Pseudogulbenkiania* sp Strain 2002. *Geochim. Cosmochim. Acta* **119**, 231–247.

Zhu-Barker X., Cavazos A. R., Ostrom N. E., Horwath W. R. and Glass J. B. (2015) The importance of abiotic reactions for nitrous oxide production. *Biogeochemistry* **126**, 251–267.

Associate editor: Hailiang Dong